17. Monitoring Process Variability Using EWMA

During the last decade, the use of the exponentially weighted moving average (EWMA) statistic as a process-monitoring tool has become more and more popular in the statistical process-control field. If the properties and design strategies of the EWMA control chart for the mean have been thoroughly investigated, the use of the EWMA as a tool for monitoring process variability has received little attention in the literature. The goal of this chapter is to present some recent innovative EWMA-type control charts for the monitoring of process variability (i. e. the sample variance, sample standard-deviation and the range). In the first section of this chapter, the definition of an EWMA sequence and its main properties will be presented together with the commonly used procedures for the numerical computation of the average run length (ARL). The second section will be dedicated to the use of the EWMA as a monitoring tool for the process position, i. e. sample mean and sample median. In the third section, the use of the EWMA for monitoring the sample variance, sample standard deviation and the range will be presented, assuming a fixed sampling interval (FSI) strategy. Finally, in the fourth section of this chapter, the variable sampling interval adaptive version of the EWMA-S^2 and EWMA-R control charts will be presented.

During the last decade, the use of the exponentially weighted moving average (EWMA) statistic as a process monitoring tool has become increasingly popular in the field of statistical process control (SPC). If the properties and design strategies of the EWMA control chart for the mean (introduced by *Roberts* [17.1]) have been thoroughly investigated by *Robinson* and *Ho* [17.2], *Crowder* [17.3] [17.4], *Lucas* and *Saccucci* [17.5] and *Steiner* [17.6], the use of the EWMA as a tool for monitoring the process variability has received little attention in the literature. Some exceptions are the papers by *Wortham* and *Ringer* [17.7], *Sweet* [17.8], *Ng* and *Case* [17.9], *Crowder* and *Hamilton* [17.10], *Hamilton* and *Crowder* [17.11] and *MacGregor* and *Harris* [17.12], *Gan* [17.13], *Amin* et al. [17.14], *Lu* and *Reynolds* [17.15], *Acosta-Mejia* et al. [17.16] and *Castagliola* [17.17]. The goal of this chapter is to present some recent innovative EWMA-type control charts for the monitoring of process variability (i. e. the sample variance, sample standard deviation and the range). From an industrial perspective, the potential of EWMA charts is important. Since their pioneer applications, these charts have proved highly sensitivity in the detection of small shifts in the monitored process parameter, due to the structure of the plotted EWMA statistic, which takes into account the past history of the process at each sampling time: this allowed them to be considered as valuable alternatives to the standard Shewhart charts, especially when the sample data needed to determine the EWMA statistic can be collected individually and evaluated automatically. As a consequence, the EWMAs have been implemented successfully on continuous processes such as those in chemical or food industries, where data involving operating variables such as temperatures, pressures, viscosity, etc. can be gathered and represented on the chart directly by the control system for the process. In the recent years, thanks to the development of simple quality-control software tools, that can be easily managed by workers and implemented on a common PC or notebook, use of EWMAs has systematically been extended to processes for manufacturing discrete parts; in this case, EWMAs that consider sample statistics like mean, median or sample variance are particularly well suited. Therefore, EWMA charts for monitoring process mean or dispersion have been successfully implemented in the semiconductor industry at the level of wafer fabrication; these processes are characterized by an extremely high level of precision in critical dimensions of parts and therefore there is the need of a statistical tool that is able to identify very small drifts in the process parameter to avoid the rejection of the product at the testing stage or, in the worst case, during the operating conditions, i.e., when the electronic device has been installed on highly expensive boards. Other applications of EWMAs to manufacturing processes involve the assembly operations in automotive industry, the technological processes involving the production of mechanical parts like CNC operations on machining centers, where process variability should be maintained as small as possible, and many others. Finally, it is important to note how EWMAs are also spreading in service control activities; an interesting example is represented by recent applications of EWMA charts to monitor healthcare outcomes such as the occurrence of infections or mortality rate after surgeries. Finally, EWMA charts can be adopted for any manufacturing process or service with a low effort and should always be preferred to Shewhart charts when there is the need to detect small shifts in the process parameters, as will be proven later in this chapter.

Therefore, in the second section of this chapter the definition of an EWMA sequence and its main properties will be presented together with the commonly used procedures for the numerical computation of the average run length (ARL). An important part of this section will focus on the numerical computation of the average run length (ARL). The third section will be dedicated to the use of the EWMA as a monitoring tool for the process position, i. e. sample mean (EWMA-$\bar{X}$) and sample median (EWMA-$\tilde{X}$). In the fourth section, the use of the EWMA for monitoring the sample variance (EWMA-S^2), sample standard deviation (EWMA-S) and the range (EWMA-R) will be presented, assuming a fixed sampling interval (FSI) strategy. In the fifth section the variable sampling interval adaptive version of the EWMA-S^2 and EWMA-R control charts will be presented.

The following notations are used – *ARL*: average run length; *ATS*: average time to signal, h_S, h_L: short and long sampling interval; K: width of the control limits; λ: EWMA smoothing parameter; *LCL*, *UCL*: lower and upper control limits; *LWL*, *UWL*: lower and upper warning limits; μ_0, σ_0: in-control mean and standard deviation; μ_1, σ_1: out-of-control mean and standard deviation; R, S, S^2: range, sample standard deviation and sample variance; τ: shift in the process position or dispersion; W: width of the warning limits; $\bar{X}$, $\tilde{X}$: sample mean and sample median.

17.1 Definition and Properties of EWMA Sequences

17.1.1 Definition

Let $T_1, \ldots, T_k, \ldots$ be a sequence of independently and identically distributed (i.i.d.) random variables and let $\lambda \in [0, 1]$ be a constant. From the sequence $T_1, \ldots, T_k, \ldots$ we define a new sequence $Y_1, \ldots, Y_k, \ldots$ using the following recurrence formula

$$Y_k = (1-\lambda)Y_{k-1} + \lambda T_k \,.$$

By decomposing Y_{k-1} in terms of Y_{k-2}, and Y_{k-2} in terms of Y_{k-3} and so on, it is straightforward to demonstrate that

$$Y_k = (1-\lambda)^k Y_0 + \lambda \sum_{j=0}^{k-1} (1-\lambda)^j T_{k-j} \,. \qquad (17.1)$$

This formula clearly shows that Y_k is a linear combination of the initial random variable Y_0 weighted by a coefficient $(1-\lambda)^k$ and the random variables $T_1, \ldots, T_k$ weighted by the coefficients $\lambda(1-\lambda)^{k-1}, \lambda(1-\lambda)^{k-2}, \ldots, \lambda$. For this reason, the sequence $Y_1, \ldots, Y_k, \ldots$ is called an exponentially weighted moving average (EWMA) sequence. If the random variables $T_1, \ldots, T_k, \ldots$ are, by definition, independent, the random variables $Y_1, \ldots, Y_k, \ldots$ are, by definition, not independent. We can notice that

- when $\lambda \to 0$ the sequence $Y_1, \ldots, Y_k, \ldots$ tends to be a smoothed version of the initial sequence $T_1, \ldots, T_k, \ldots$. When $\lambda = 0$ we have $Y_k = Y_{k-1} = \cdots = Y_0$.
- when $\lambda \to 1$ the sequence $Y_1, \ldots, Y_k, \ldots$ tends to be a copy of the initial sequence $T_1, \ldots, T_k, \ldots$ When $\lambda = 1$ we have $Y_k = T_k$ for $k \geq 1$.

17.1.2 Expectation and Variance of EWMA Sequences

Let $\mu_T = E(T_k)$ and $\sigma_T^2 = V(T_k)$ be the expectation and the variance of the random variables $T_1, \ldots, T_k, \ldots$ Using (17.1), we find that the expected value of the random variable Y_k is:

$$E(Y_k) = (1-\lambda)^k E(Y_0) + \lambda \mu_T \sum_{j=0}^{k-1} (1-\lambda)^j$$

or, equivalently, that

$$E(Y_k) = (1-\lambda)^k E(Y_0) + \mu_T [1 - (1-\lambda)^k] .$$

Assuming $E(Y_0) = \mu_T$, for $k \geq 1$ it results that

$$E(Y_k) = \mu_T .$$

Because the random variables $T_1, T_2, \ldots$ are supposed to be independent, the variance $V(Y_k)$ of the random variable Y_k is

$$V(Y_k) = (1-\lambda)^{2k} V(Y_0) + \lambda^2 \sigma_T^2 \sum_{j=0}^{k-1} (1-\lambda)^{2j} .$$

Replacing $\sum_{j=0}^{k-1}(1-\lambda)^{2j}$ by $[1-(1-\lambda)^{2k}]/[\lambda(2-\lambda)]$ gives

$$V(Y_k) = (1-\lambda)^{2k} V(Y_0) + \lambda^2 \sigma_T^2 \left(\frac{1-(1-\lambda)^{2k}}{\lambda(2-\lambda)} \right) .$$

Finally, after some simplifications, we have

$$V(Y_k) = (1-\lambda)^{2k} V(Y_0) + \left(\frac{\lambda}{2-\lambda} \right) [1-(1-\lambda)^{2k}] \sigma_T^2 .$$

Two common assumptions can be made to determine the variance $V(Y_0)$ of the initial random variable Y_0:

- If we assume $V(Y_0) = 0$ (i. e., $Y_0 = \mu_T$ is a constant) then we have, for $k \geq 1$,

$$V(Y_k) = \left(\frac{\lambda}{2-\lambda} \right) [1-(1-\lambda)^{2k}] \sigma_T^2 .$$

- If we assume $V(Y_0) = \sigma_T^2$ then we have, for $k \geq 1$,

$$V(Y_k) = \left(\frac{\lambda + 2(1-\lambda)^{2k+1}}{2-\lambda} \right) \sigma_T^2 .$$

For either choice $V(Y_0) = 0$ or $V(Y_0) = \sigma_T^2$, the asymptotic variance $V_\infty(Y_k)$ of the random variable Y_k is

$$V_\infty(Y_k) = \lim_{k \to +\infty} V(Y_k) = \left(\frac{\lambda}{2-\lambda} \right) \sigma_T^2 .$$

17.1.3 The ARL for an EWMA Sequence

Let LCL and UCL be two constants satisfying $LCL < \mu_T < UCL$. Let $f_T(t)$ and $F_T(t)$ be the probability density function (p.d.f.) and the cumulative distribution function (c.d.f.) of the random variables $T_1, \ldots, T_k, \ldots$ Because the random variables $T_1, \ldots, T_k, \ldots$ are assumed to be independent, the average run length ARL_T for the sequence $T_1, \ldots, T_k, \ldots$ is given by

$$ARL_T = \frac{1}{F_T(LCL) + 1 - F_T(UCL)} . \tag{17.2}$$

Let $ARL_Y(y)$ be the average run length of the EWMA sequence $Y_1, \ldots, Y_k, \ldots$ assuming $Y_0 = y$ and let $ARL_Y = ARL_Y(\mu_T)$. The fact that the random variables $Y_1, \ldots, Y_k, \ldots$ are not independent prevents the use of (17.2) for computing $ARL_Y(y)$. There are two main approaches for computing ARL_Y.

The first approach is based on the fact that $ARL_Y(y)$ must satisfy the following equation

$$ARL_Y(y) = 1 + \int_{LCL}^{UCL} \frac{1}{\lambda} \times f_T\left(\frac{z-(1-\lambda)y}{\lambda} \right) ARL_Y(z) \mathrm{d}z .$$

This equation is a Fredholm equation of the second kind, i. e.

$$f(y) = g(y) + \int_{z_1}^{z_n} h(y, z) f(z) \mathrm{d}z ,$$

where $h(y, z)$ and $g(y)$ are two known functions and where $f(z)$ is an unknown function that satisfies the equation above. In our case, we have $g(y) = 1$, $h(y, z) = f_T[z - (1-\lambda)y]/\lambda/\lambda$ and $f(y) = ARL_Y(y)$. The numerical evaluation of a Fredholm equation (see *Press* et al. [17.18]) of the second kind consists of approximating the integral operand by a weighted sum

$$f(y) \simeq g(y) + \sum_{i=1}^{n} w_i h(y, z_i) f(z_i) , \tag{17.3}$$

where $z_1, z_2, \dots, z_n$ and $w_1, w_2, \dots, w_n$ are, respectively, the abscissas and weights of a quadrature method on $[z_1, z_n]$ such as, for instance, the n-point Gauss–Legendre quadrature. If we apply (17.3) for $y = z_1, z_2, \dots, z_n$, we have

$$\begin{aligned} f_1 &\simeq g_1 + w_1 h_{1,1} f_1 + w_2 h_{1,2} f_2 + \dots + w_n h_{1,n} f_n , \\ f_2 &\simeq g_2 + w_1 h_{2,1} f_1 + w_2 h_{2,2} f_2 + \dots + w_n h_{2,n} f_n , \\ &\vdots \\ f_n &\simeq g_n + w_1 h_{n,1} f_1 + w_2 h_{n,2} f_2 + \dots + w_n h_{n,n} f_n , \end{aligned}$$

where $f_i = f(z_i)$, $g_i = g(z_i)$ and $h_{i,j} = h(z_i, z_j)$. This set of equations can be rewritten in a matrix form

$$\begin{pmatrix} f_1 \\ f_2 \\ \vdots \\ f_n \end{pmatrix} \simeq \begin{pmatrix} g_1 \\ g_2 \\ \vdots \\ g_n \end{pmatrix} + \begin{pmatrix} w_1 h_{1,1} & w_2 h_{1,2} & \cdots & w_n h_{1,n} \\ w_1 h_{2,1} & w_2 h_{2,2} & \cdots & w_n h_{2,n} \\ \vdots & \vdots & \ddots & \vdots \\ w_1 h_{n,1} & w_2 h_{n,2} & \cdots & w_n h_{n,n} \end{pmatrix} \begin{pmatrix} f_1 \\ f_2 \\ \vdots \\ f_n \end{pmatrix}$$

or in a more compact way as

$$\boldsymbol{f} \simeq \boldsymbol{g} + \mathbf{H}\boldsymbol{f} .$$

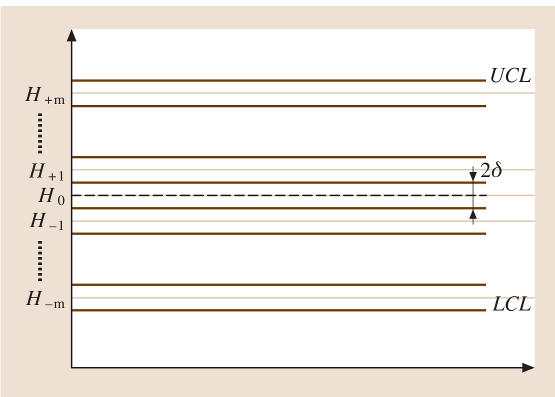

Fig. 17.1 Interval between *LCL* and *UCL* divided into $p = 2m+1$ subintervals of width 2δ

Solving the equation above for $\boldsymbol{f}$, we obtain $(\mathbf{I} - \mathbf{H})\boldsymbol{f} \simeq \boldsymbol{g}$, and finally

$$\boldsymbol{f} \simeq (\mathbf{I} - \mathbf{H})^{-1} \boldsymbol{g} .$$

The second approach is based on the flexible and relatively easy to use Markov-chain approach, originally proposed by *Brook* and *Evans* [17.19]. This procedure involves dividing the interval between *LCL* and *UCL* (Fig. 17.1) into $p = 2m+1$ subintervals of width 2δ, where $\delta = (UCL - LCL)/(2p)$. When the number of subintervals p is sufficiently large, the finite approach provides an effective method that allows ARL_Y to be accurately evaluated. The statistic $Y_k = (1-\lambda)Y_{k-1} + \lambda T_k$ is said to be in *transient state* j at time k if $H_j - \delta < Y_k < H_j + \delta$ for $j = -m, \dots, -1, 0, +1, \dots, m$, where H_j represents the midpoint of the j-th subinterval. The statistic Y_k is in the *absorbing state* if $Y_k \notin [LCL, UCL]$. An approximation for ARL_Y is given by

$$ARL_Y \simeq \boldsymbol{d}^{\mathrm{T}} \mathbf{Q} \boldsymbol{g} ,$$

where $\boldsymbol{d}$ is the $(p, 1)$ initial probability vector, $\mathbf{Q} = (\mathbf{I} - \mathbf{P})^{-1}$ is the fundamental (p, p) matrix, $\mathbf{P}$ is the (p, p) transition-probabilities matrix and $\boldsymbol{g} = \boldsymbol{1}$ is a $(p, 1)$ vector of 1s. The initial probability vector $\boldsymbol{d}$ contains the probabilities that the statistic Y_k starts in a given state. This vector is such that, for $j = -m, \dots, -1, 0, +1, \dots, m$,

$$d_j = \begin{cases} 1 & \text{if } H_j - \delta < Y_0 < H_j + \delta \\ 0 & \text{otherwise} . \end{cases}$$

This vector contains a single entry equal to 1, whereas its $2m$ remaining elements are all equal to 0. The transition-probability matrix $\mathbf{P}$ contains the one-step transition probabilities. The generic element $p_{i,j}$ of $\mathbf{P}$ represents the probability that the statistic Y_k goes from state i to state j in one step. In order to approximate this probability, it is assumed that the statistic Y_k is equal to H_j whenever it is in state j, i. e.

$$\begin{aligned} p_{i,j} \simeq P\Bigg(& \frac{H_j - \delta - (1-\lambda)H_i}{\lambda} < T_k \\ & < \frac{H_j + \delta - (1-\lambda)H_i}{\lambda} \Bigg) . \end{aligned}$$

This probability can be rewritten

$$\begin{aligned} p_{i,j} \simeq\, & F_T\left(\frac{H_j + \delta - (1-\lambda)H_i}{\lambda} \right) \\ & - F_T\left(\frac{H_j - \delta - (1-\lambda)H_i}{\lambda} \right) . \end{aligned}$$

17.2 EWMA Control Charts for Process Position

17.2.1 EWMA-$\bar{X}$ Control Chart

Let $X_{k,1}, \ldots, X_{k,n}$ be a sample of n independent normal (μ_0, σ_0) random variables, where μ_0 is the nominal process mean, σ_0 is the nominal process standard deviation and k is the subgroup number. Let $\bar{X}_k$ be the sample mean of subgroup k, i. e.,

$$\bar{X}_k = \frac{1}{n} \sum_{j=1}^{n} X_{k,j} \, .$$

Traditional Shewhart control charts $(\bar{X}, R)$ or $(\bar{X}, S)$ directly monitor the sample mean $\bar{X}_k$, in contrast to EWMA-$\bar{X}$ control charts, which monitor the statistic $Y_k = (1-\lambda)Y_{k-1} + \lambda \bar{X}_k$, i. e., $T_k = \bar{X}_k$. This implies that $\mu_T = \mu_0$ and $\sigma_T = \sigma_0/\sqrt{n}$ and, consequently, the (fixed) control limits of the EWMA-$\bar{X}$ control chart (introduced by *Roberts* [17.1]) are

$$LCL = \mu_0 - K\sqrt{\frac{\lambda}{2-\lambda}} \frac{\sigma_0}{\sqrt{n}} \, ,$$

$$UCL = \mu_0 + K\sqrt{\frac{\lambda}{2-\lambda}} \frac{\sigma_0}{\sqrt{n}} \, ,$$

where K is a positive constant.

Example 17.1: Figure 17.2 reports a simulation of 200 data obtained from a manufacturing process: the 150 first data plotted in Fig. 17.2 consist of $m = 30$ subgroups of $n = 5$ observations randomly generated from a normal $(\mu_0 = 20, \sigma_0 = 0.1)$ distribution; the remaining 50 data are collected within 10 subgroups of $n = 5$ observations randomly generated from a normal (20.05, 0.1) distribution: that is, the process position was shifted up by half the nominal standard deviation. The process mean and standard deviation were estimated by considering the subgroups $1, \ldots, 30$, corresponding to the in-control condition: $\hat{\mu}_0 = 19.99$, $\hat{\sigma}_0 = 0.099$. Assuming $K = 3$, the control limits of the EWMA chart are, respectively, equal to:

- if $\lambda = 0.1$, $LCL = 19.959$ and $UCL = 20.020$,
- if $\lambda = 0.3$, $LCL = 19.934$ and $UCL = 20.046$.

In Fig. 17.3, we plot the EWMA-$\bar{X}$ control charts for the cases $\lambda = 0.1$ and $\lambda = 0.3$. We can see that these control charts detect an out-of-control signal at the 34-th subgroup (in the case $\lambda = 0.1$) and at the 33-rd subgroup (in the case $\lambda = 0.3$), point-

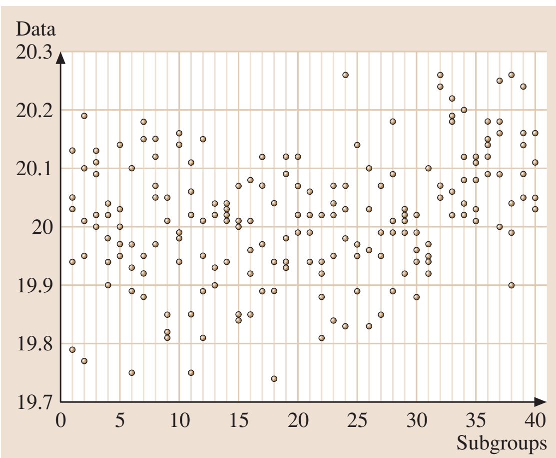

Fig. 17.2 Data with a half-standard-deviation shift in the process mean/median

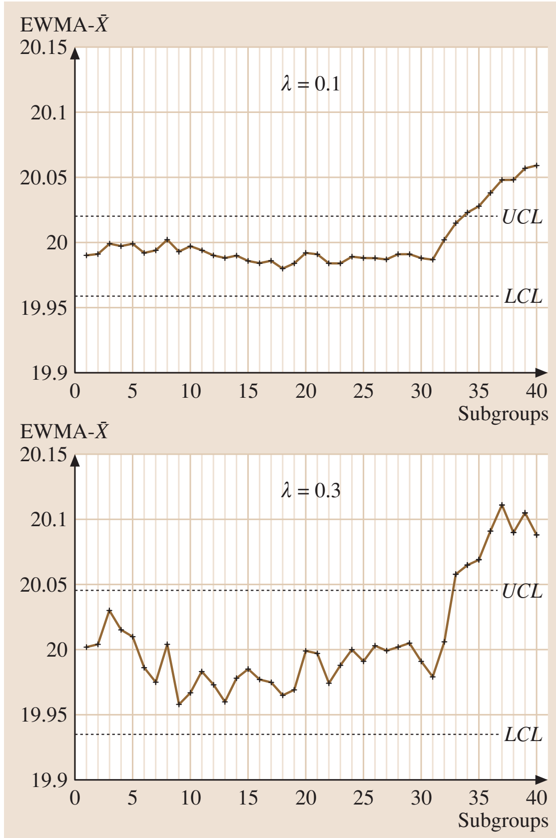

Fig. 17.3 EWMA-$\bar{X}$ control charts corresponding to the data in Fig. 17.2 for $\lambda = 0.1$ and $\lambda = 0.3$

ing out that an increasing of the process position occurred.

17.2.2 EWMA-$\tilde{X}$ Control Chart

Let $X_{k,(1)}, \ldots, X_{k,(n)}$ be the ordered sample corresponding to $X_{k,1}, \ldots, X_{k,n}$ and let $\tilde{X}_k$ be the sample median of subgroup k, i. e.

$$\tilde{X}_k = \begin{cases} X_{k,[(n+1)/2]} & \text{if } n \text{ is odd} \\ \dfrac{X_{k,(n/2)} + X_{k,(n/2+1)}}{2} & \text{if } n \text{ is even}\,. \end{cases}$$

The EWMA-$\tilde{X}$ control chart is a natural extension of the EWMA-$\bar{X}$ control chart investigated by *Castagliola* [17.20] where the monitored statistic is $Y_k = (1-\lambda)Y_{k-1} + \lambda\tilde{X}_k$, i. e., $T_k = \tilde{X}_k$. The (fixed) control limits of the EWMA-$\tilde{X}$ control chart are

$$LCL = \mu_0 - K\sqrt{\frac{\lambda}{2-\lambda}}\sigma(\tilde{X})\,,$$

$$UCL = \mu_0 + K\sqrt{\frac{\lambda}{2-\lambda}}\sigma(\tilde{X})\,,$$

where $\sigma(\tilde{X})$ is the standard deviation of the sample median $\tilde{X}$. It is straightforward to show that $\sigma(\tilde{X}) = \sigma_0 \times \sigma(\tilde{Z})$ where $\sigma(\tilde{Z})$ is the standard deviation of the normal (0, 1) sample median. The values of $\sigma(\tilde{Z})$ are tabulated in Table 17.1 for $n \in \{3, 5, \ldots, 25\}$, but they can also be computed, when n is odd, (see *Castagliola* [17.21]), using the following approximation

$$\sigma(\tilde{Z}) \simeq \sqrt{\frac{\pi}{2(n+2)} + \frac{\pi^2}{4(n+2)^2} + \frac{\pi^2(\frac{13}{24}\pi - 1)}{2(n+2)^3}}\,.$$

Table 17.1 Standard-deviation $\sigma(\tilde{Z})$ of the normal (0, 1) sample median, for $n \in \{3, 5, \ldots, 25\}$

n	$\sigma(\tilde{Z})$
3	0.6698
5	0.5356
7	0.4587
9	0.4076
11	0.3704
13	0.3418
15	0.3189
17	0.3001
19	0.2842
21	0.2707
23	0.2589
25	0.2485

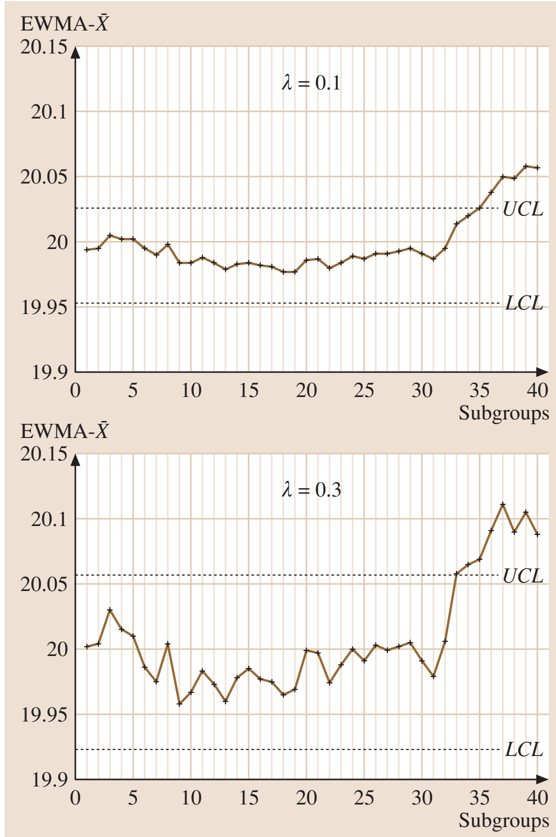

Fig. 17.4 EWMA-$\tilde{X}$ control charts corresponding to the data in Fig. 17.2 for $\lambda = 0.1$ and $\lambda = 0.3$

Example 17.2: using the same data (Fig. 17.2) as in the previous example, we computed the control limits of the EWMA-$\tilde{X}$ control chart ($K = 3$ assumed)

- if $\lambda = 0.1$, $LCL = 19.953$ and $UCL = 20.026$,
- if $\lambda = 0.3$, $LCL = 19.923$ and $UCL = 20.057$.

In Fig. 17.4 we plot the EWMA-$\tilde{X}$ control charts for the cases $\lambda = 0.1$ and $\lambda = 0.3$. Similarly to the EWMA-$\bar{X}$ control charts, we can see that these control charts detect an out-of-control signal at the 36-th subgroup (in the case $\lambda = 0.1$) and at the 33-rd subgroup (in the case $\lambda = 0.3$), pointing out again that an increasing of the process position occurred.

17.2.3 ARL Optimization for the EWMA-$\bar{X}$ and EWMA-$\tilde{X}$ Control Charts

Let $\tau = |\mu_1 - \mu_0|/\sigma_0$ be the usual variable reflecting the shift in the process position, where μ_1 is the new out-

Table 17.2 Optimal couples (λ^*, K^*) and optimal ARL^* of the EWMA-$\bar{X}$ (*half top*) and EWMA-$\tilde{X}$ (*half bottom*) control charts, for $\tau \in \{0.1, 0.2, \dots, 2\}$, $n \in \{1, 3, 5, 7, 9\}$ and $ARL_0 = 370.4$

EWMA-$\bar{X}$																				
τ	$n=1$				$n=3$				$n=5$				$n=7$				$n=9$			
	λ^*	K^*	ARL^*	$\bar{X}$	λ^*	K^*	ARL^*	$\bar{X}$	λ^*	K^*	ARL^*	$\bar{X}$	λ^*	K^*	ARL^*	$\bar{X}$	λ^*	K^*	ARL^*	$\bar{X}$
0.1	0.01	1.824	183.0	352.9	0.01	1.824	103.5	322.1	0.02	2.139	77.1	295.8	0.02	2.139	62.2	273.0	0.02	2.139	53.1	253.1
0.2	0.01	1.824	87.8	308.4	0.03	2.305	43.9	227.7	0.04	2.414	31.0	177.7	0.05	2.492	24.5	143.9	0.07	2.601	20.4	119.7
0.3	0.02	2.139	53.1	253.1	0.05	2.492	25.1	147.5	0.08	2.640	17.4	99.5	0.10	2.703	13.5	72.7	0.12	2.749	11.2	55.8
0.4	0.04	2.414	36.2	200.1	0.08	2.640	16.6	94.0	0.12	2.749	11.3	56.6	0.15	2.801	8.8	38.3	0.18	2.840	7.3	27.8
0.5	0.05	2.492	26.5	155.2	0.11	2.727	11.9	60.7	0.17	2.828	8.1	33.4	0.21	2.869	6.3	21.4	0.25	2.898	5.2	15.0
0.6	0.07	2.601	20.4	119.7	0.15	2.801	9.0	40.0	0.22	2.877	6.1	20.6	0.28	2.916	4.7	12.7	0.33	2.938	3.9	8.7
0.7	0.08	2.640	16.3	92.3	0.19	2.850	7.2	27.1	0.27	2.910	4.9	13.2	0.34	2.941	3.8	8.0	0.41	2.962	3.1	5.4
0.8	0.10	2.703	13.4	71.6	0.23	2.885	5.8	18.8	0.33	2.938	4.0	8.9	0.42	2.964	3.1	5.3	0.51	2.979	2.5	3.6
0.9	0.12	2.749	11.2	55.8	0.27	2.910	4.9	13.4	0.39	2.957	3.3	6.2	0.50	2.978	2.6	3.7	0.61	2.989	2.1	2.6
1.0	0.14	2.786	9.6	43.9	0.31	2.930	4.2	9.8	0.46	2.972	2.8	4.5	0.59	2.988	2.2	2.8	0.70	2.995	1.8	2.0
1.1	0.16	2.815	8.3	34.8	0.36	2.948	3.6	7.3	0.53	2.982	2.4	3.4	0.67	2.993	1.9	2.2	0.77	2.997	1.5	1.6
1.2	0.18	2.840	7.3	27.8	0.41	2.962	3.2	5.6	0.60	2.989	2.1	2.7	0.74	2.996	1.6	1.8	0.83	2.999	1.3	1.4
1.3	0.21	2.869	6.4	22.4	0.46	2.972	2.8	4.4	0.67	2.993	1.9	2.2	0.80	2.998	1.4	1.5	0.88	2.999	1.2	1.2
1.4	0.23	2.885	5.7	18.2	0.52	2.981	2.5	3.5	0.73	2.996	1.7	1.8	0.85	2.999	1.3	1.3	0.92	3.000	1.1	1.1
1.5	0.25	2.898	5.2	15.0	0.58	2.987	2.2	2.9	0.79	2.998	1.5	1.6	0.89	2.999	1.2	1.2	0.95	3.000	1.1	1.1
1.6	0.28	2.916	4.7	12.4	0.63	2.991	2.0	2.4	0.83	2.999	1.4	1.4	0.93	3.000	1.1	1.1	0.97	3.000	1.0	1.0
1.7	0.30	2.925	4.3	10.3	0.68	2.994	1.8	2.1	0.87	2.999	1.3	1.3	0.95	3.000	1.1	1.1	0.99	3.000	1.0	1.0
1.8	0.33	2.938	3.9	8.7	0.73	2.996	1.7	1.8	0.90	3.000	1.2	1.2	0.97	3.000	1.0	1.0	0.99	3.000	1.0	1.0
1.9	0.36	2.948	3.6	7.4	0.77	2.997	1.5	1.6	0.93	3.000	1.1	1.1	0.98	3.000	1.0	1.0	1.00	3.000	1.0	1.0
2.0	0.38	2.954	3.3	6.3	0.81	2.998	1.4	1.5	0.95	3.000	1.1	1.1	0.99	3.000	1.0	1.0	1.00	3.000	1.0	1.0
0.1	0.01	1.824	183.0	352.9	0.01	2.116	122.1	335.2	0.01	2.184	95.0	317.7	0.01	2.214	79.5	301.4	0.02	2.615	68.5	286.3
0.2	0.01	1.824	87.8	308.4	0.02	2.481	53.4	258.3	0.03	2.760	39.7	218.3	0.04	2.930	32.1	187.2	0.05	3.047	27.2	162.6
0.3	0.02	2.139	53.1	253.1	0.04	2.800	30.9	182.6	0.06	3.057	22.6	137.4	0.07	3.157	18.0	107.5	0.09	3.270	15.2	86.8
0.4	0.04	2.414	36.2	200.1	0.07	3.018	20.6	125.2	0.09	3.204	14.8	85.4	0.11	3.312	11.8	62.2	0.14	3.409	9.9	47.5
0.5	0.05	2.492	26.5	155.2	0.09	3.104	14.9	85.7	0.13	3.318	10.6	53.9	0.16	3.420	8.4	37.1	0.19	3.488	7.0	27.2
0.6	0.07	2.601	20.4	119.7	0.12	3.192	11.3	59.2	0.17	3.391	8.1	34.9	0.21	3.487	6.4	23.0	0.24	3.541	5.3	16.4
0.7	0.08	2.640	16.3	92.3	0.15	3.254	9.0	41.6	0.21	3.441	6.4	23.2	0.26	3.532	5.1	14.8	0.30	3.583	4.2	10.4
0.8	0.10	2.703	13.4	71.6	0.18	3.299	7.3	29.7	0.25	3.478	5.2	15.9	0.31	3.564	4.1	9.9	0.37	3.617	3.5	6.9
0.9	0.12	2.749	11.2	55.8	0.21	3.334	6.1	21.6	0.29	3.506	4.4	11.2	0.37	3.592	3.5	6.9	0.44	3.640	2.9	4.8
1.0	0.14	2.786	9.6	43.9	0.25	3.370	5.2	16.0	0.34	3.533	3.7	8.1	0.43	3.612	3.0	5.0	0.52	3.657	2.5	3.5
1.1	0.16	2.815	8.3	34.8	0.28	3.391	4.5	12.0	0.39	3.553	3.2	6.0	0.50	3.629	2.6	3.8	0.60	3.669	2.1	2.7
1.2	0.18	2.840	7.3	27.8	0.32	3.414	4.0	9.2	0.45	3.572	2.8	4.6	0.57	3.641	2.2	2.9	0.67	3.677	1.8	2.1
1.3	0.21	2.869	6.4	22.4	0.36	3.432	3.5	7.2	0.51	3.585	2.5	3.6	0.64	3.650	2.0	2.3	0.74	3.682	1.6	1.8
1.4	0.23	2.885	5.7	18.2	0.40	3.447	3.2	5.7	0.57	3.595	2.2	2.9	0.70	3.655	1.7	2.0	0.80	3.685	1.4	1.5
1.5	0.25	2.898	5.2	15.0	0.45	3.461	2.8	4.6	0.63	3.603	2.0	2.4	0.76	3.659	1.6	1.7	0.84	3.687	1.3	1.3
1.6	0.28	2.916	4.7	12.4	0.49	3.470	2.6	3.8	0.68	3.608	1.8	2.1	0.81	3.662	1.4	1.5	0.88	3.688	1.2	1.2
1.7	0.30	2.925	4.3	10.3	0.54	3.480	2.3	3.2	0.73	3.612	1.6	1.8	0.85	3.663	1.3	1.3	0.92	3.688	1.1	1.1
1.8	0.33	2.938	3.9	8.7	0.59	3.487	2.1	2.7	0.78	3.615	1.5	1.6	0.88	3.664	1.2	1.2	0.94	3.689	1.1	1.1
1.9	0.36	2.948	3.6	7.4	0.64	3.493	2.0	2.4	0.82	3.617	1.4	1.4	0.91	3.665	1.1	1.2	0.96	3.689	1.1	1.1
2.0	0.38	2.954	3.3	6.3	0.68	3.497	1.8	2.1	0.85	3.618	1.3	1.3	0.94	3.665	1.1	1.1	0.98	3.689	1.0	1.0

of-control process position. The *ARL* of the EWMA-$\bar{X}$ and EWMA-$\tilde{X}$ control charts can be computed using one of the methods presented in Sect. 17.2.3. The p.d.f and c.d.f. $f_T(t)$ and $F_T(t)$, required for the computation of ARL_Y, are

- for the EWMA-$\bar{X}$ control chart

$$f_T(t) = \sqrt{n}\phi[(t-\tau)\sqrt{n}]$$
$$F_T(t) = \Phi[(t-\tau)\sqrt{n}]$$

  where $\phi(x)$ and $\Phi(x)$ are the p.d.f. and the c.d.f. of the normal (0, 1) distribution.
- for the EWMA-$\tilde{X}$ control chart

$$f_T(t) = \phi(t-\tau) f_\beta\left[\Phi(t-\tau)|\frac{n+1}{2}, \frac{n+1}{2}\right],$$
$$F_T(t) = F_\beta\left[\Phi(t-\tau)|\frac{n+1}{2}, \frac{n+1}{2}\right],$$

  where $f_\beta(x|a,b)$ and $F_\beta(x|a,b)$ are the p.d.f. and the c.d.f. of the (a,b) beta distribution.

The quality practitioner should be interested in determining the optimal couples (λ^*, K^*) that allow one to achieve:

- $ARL_Y = ARL_0$, where ARL_0 is the in-control *ARL*, corresponding to the process functioning at nominal position $\mu = \mu_0$, that is to $\tau = 0$;
- A minimum value for the out-of-control *ARL*, $ARL_Y = ARL_Y^*$, valid when $\tau > 0$.

Each couple (λ^*, K^*) is then optimally designed for detecting a particular shift τ. We chose to take $ARL_0 = 370.4$ for the in-control *ARL* (corresponding to the classical 3σ Shewhart control limits). In order to compute the couples (λ^*, K^*), we adopted the following approach

1. For every $\lambda \in \{0.01, 0.02, \dots, 1\}$ and for $\tau = 0$, we computed (using a basic Newton-type algorithm) the corresponding value K such that $ARL_Y = ARL_0$. At the end of this step, we have a set of pairs $\{(0.01, K_{0.01}), (0.02, K_{0.02}), \dots, (1, K_1)\}$ candidating for the second step.
2. For every shift $\tau \in \{0.1, 0.2, \dots, 2\}$, and for every pair $\{(0.01, K_{0.01}), (0.02, K_{0.02}), \dots, (1, K_1)\}$ we computed ARL_Y and chose the pair (λ^*, K^*) that gave the minimum $ARL_Y = ARL_Y^*$.

The optimal couples (λ^*, K^*) and the corresponding minimal ARL^* are shown in Table 17.2, for both the EWMA-$\bar{X}$ and EWMA-$\tilde{X}$ control charts. In Table 17.2, we also added, for comparison purpose, the *ARL* of the Shewhart $\bar{X}$ and $\tilde{X}$ control charts. For example, the optimal couple (λ^*, K^*) ensuring the smallest *ARL* for a shift $\tau = 0.5$ and $n = 7$ are (0.21, 2.869) for the EWMA-$\bar{X}$ control chart and (0.16, 3.420) for the EWMA-$\tilde{X}$ control chart. In that case, the minimal *ARL* is $ARL^* = 6.3$ for the EWMA-$\bar{X}$ control chart ($ARL = 21.4$ for the $\bar{X}$ control chart) and $ARL^* = 8.4$ for the EWMA-$\tilde{X}$ control chart ($ARL = 37.1$ for the $\tilde{X}$ control chart). Table 17.2 clearly demonstrates that, in terms of *ARL*, the EWMA-$\bar{X}$ control chart is more efficient than the EWMA-$\tilde{X}$ control chart and both the EWMA-$\bar{X}$ and EWMA-$\tilde{X}$ control charts are more efficient, for small and medium shift, than the traditional $\bar{X}$ and $\tilde{X}$ control charts.

17.3 EWMA Control Charts for Process Dispersion

17.3.1 EWMA-S^2 Control Chart

Let S_k^2 be the sample variance of subgroup k, i. e.,

$$S_k^2 = \frac{1}{n-1}\sum_{j=1}^{n}(X_{k,j} - \bar{X}_k)^2,$$

where $\bar{X}_k$ is the sample mean of subgroup k. In order to monitor the process variance, *Crowder* and *Hamilton* [17.10], following a recommendation by *Box* [17.22], suggested the application of the classical EWMA approach to the logarithm of the successive sample variances, i. e. $T_k = \ln S_k^2$. The main motivation for this approach is that $T_k = \ln S_k^2$, which has a log-gamma distribution (*Johnson* et al. [17.23]), tends to be more normally distributed than the sample variance S_k^2. A more recent idea developed by *Castagliola* [17.24] was to apply a three-parameter $(a_{S^2}, b_{S^2}, c_{S^2})$ logarithmic transformation to S_k^2, i. e. $T_k = a_{S^2} + b_{S^2}\ln(S_k^2 + c_{S^2})$, with $c_{S^2} > 0$ (in order to avoid problems with the logarithmic transformation). The main expectation of this approach is that, if the parameters a_{S^2}, b_{S^2} and c_{S^2} are judiciously selected, then this transformation may result in better normality of T_k than the approach of *Crowder* and *Hamilton* [17.10]. Trying to make T_k more normally distributed is related to making the distribution of T_k more symmetric. If the value of the expectation $E(T_k)$ and the standard deviation $\sigma(T_k)$ of T_k corresponding to the parameters a_{S^2}, b_{S^2} and c_{S^2} are known, then the (fixed) control limits of the EWMA-S^2 control chart are

$$LCL = E(T_k) - K\sqrt{\frac{\lambda}{2-\lambda}}\sigma(T_k)\,, \tag{17.4}$$

$$UCL = E(T_k) + K\sqrt{\frac{\lambda}{2-\lambda}}\sigma(T_k)\,. \tag{17.5}$$

The control limits given above correspond to a two-sided EWMA control chart, but one-sided EWMA control limits can also be considered. The approach suggested by *Castagliola* [17.24] needs to define a_{S^2}, b_{S^2}, c_{S^2}, $E(T_k)$, $\sigma(T_k)$ and Y_0. Let S^2 be the sample variance of n independent normal $(\mu_0, 1)$ random variables. The p.d.f. and the c.d.f of S^2 are defined for $s \geq 0$ and are equal to

$$f_{S^2}(s) = f_\gamma\left(s|\frac{n-1}{2}, \frac{2}{n-1}\right)\,,$$

$$F_{S^2}(s) = F_\gamma\left(s|\frac{n-1}{2}, \frac{2}{n-1}\right)\,,$$

where $f_\gamma(x|u, v)$ and $F_\gamma(x|u, v)$ are the p.d.f. and c.d.f. of the gamma (u, v) distribution

$$f_\gamma(x|u,v) = \begin{cases} 0 & (x \leq 0) \\ \dfrac{x^{u-1}\exp(-x/v)}{v^u\Gamma(u)} & (x > 0)\,. \end{cases}$$

Consequently, the expectation $E(S^2)$, the variance $V(S^2)$, and the skewness coefficient $\gamma_3(S^2)$ of S^2 are equal to

$$E(S^2) = 1\,,$$

$$V(S^2) = \frac{2}{n-1}\,,$$

$$\gamma_3(S^2) = \sqrt{\frac{8}{n-1}}\,.$$

In the approach developed by *Castagliola* [17.24], three parameters $A_{S^2}(n)$, $B_{S^2}(n)$, and $C_{S^2}(n)$, depending only on n, must be computed such that $T = A_{S^2}(n) + B_{S^2}(n)\ln[S^2 + C_{S^2}(n)]$ is approximately a normal (0, 1) random variable. Remembering that S^2 has a gamma distribution, i.e. a unimodal skewed distribution, Castagliola suggested to find the three parameters log-normal distribution (another skewed distribution), defined for $x \geq -C_{S^2}(n)$,

$$f_L(x) = \frac{B_{S^2}(n)}{x}\phi\left[A_{S^2}(n) + B_{S^2}(n)\ln[x + C_{S^2}(n)]\right]\,,$$

which is the closest to the distribution of S^2, according to a criterion based on the first three moments $E(S^2)$, $V(S^2)$, and $\gamma_3(S^2)$ of S^2. If S^2 would have a log-normal distribution, then $T = A_{S^2}(n) + B_{S^2}(n)\ln[S^2 + C_{S^2}(n)]$ would have exactly a normal (0, 1) distribution. By looking for a log-normal distribution which fits approximately the (gamma) distribution of S^2, we expect that T will have an approximate normal (0, 1) distribution. What Castagliola suggested is to find parameters $A_{S^2}(n)$, $B_{S^2}(n)$, and $C_{S^2}(n)$ such that the log-normal distribution $f_L(x)$ fits the first three moments $E(S^2)$, $V(S^2)$, and $\gamma_3(S^2)$ of S^2. This can be achieved (*Stuart* and *Ord* [17.25]) by firstly computing

$$w = \left[\sqrt{\gamma_3^2(S^2)/4 + 1} + \gamma_3(S^2)/2\right]^{1/3} - \left[\sqrt{\gamma_3^2(S^2)/4 + 1} - \gamma_3(S^2)/2\right]^{1/3}$$

and then

$$B_{S^2}(n) = \frac{1}{\sqrt{\ln(w^2+1)}}\,,$$

$$A_{S^2}(n) = \frac{B_{S^2}(n)}{2}\ln\left(\frac{w^2(w^2+1)}{V(S^2)}\right)\,,$$

$$C_{S^2}(n) = \frac{\sqrt{V(S^2)}}{w} - E(S^2)\,.$$

The value of the constants $A_{S^2}(n)$, $B_{S^2}(n)$ and $C_{S^2}(n)$ can be found in Table 17.3 for $n \in \{3, \ldots, 15\}$. For the random variable $S_k^2 = \sigma_0^2 S^2$ [corresponding to the sample variance of n independent normal (μ_0, σ_0) random variables], it is straightforward to see that

$$\begin{aligned} T &= A_{S^2}(n) + B_{S^2}(n)\ln\left[S^2 + C_{S^2}(n)\right] \\ &= A_{S^2}(n) + B_{S^2}(n)\ln\left[S_k^2/\sigma_0^2 + C_{S^2}(n)\right] \\ &= A_{S^2}(n) - 2B_{S^2}(n)\ln(\sigma_0) + B_{S^2}(n)\ln\left[S_k^2 \right. \\ &\quad \left. + C_{S^2}(n)\sigma_0^2\right]. \end{aligned}$$

Consequently, if the parameters a_{S^2}, b_{S^2} and c_{S^2} are defined such that

$$b_{S^2} = B_{S^2}(n)\,,$$

$$c_{S^2} = C_{S^2}(n)\sigma_0^2\,,$$

$$a_{S^2} = A_{S^2}(n) - 2B_{S^2}(n)\ln(\sigma_0)\,,$$

then $T = a_{S^2} + b_{S^2}\ln(S_k^2 + c_{S^2}) = T_k$. This ensures that $T_k = a_{S^2} + b_{S^2}\ln(S_k^2 + c_{S^2})$ will also be approximately a normal (0, 1) random variable. Because $T_k = T$, the distribution $f_T(t)$ of T_k depends only on n. This distribution is defined for $t \geq A_{S^2}(n) + B_{S^2}(n)\ln[C_{S^2}(n)]$ and

Table 17.3 Constants $A_{S^2}(n)$, $B_{S^2}(n)$, $C_{S^2}(n)$, Y_0, $E(T_k)$, $\sigma(T_k)$, $\gamma_3(T_k)$ and $\gamma_4(T_k)$ for the EWMA-S^2 control chart, for $n \in \{3, \ldots, 15\}$

EWMA-S^2								
n	$A_{S^2}(n)$	$B_{S^2}(n)$	$C_{S^2}(n)$	Y_0	$E(T_k)$	$\sigma(T_k)$	$\gamma_3(T_k)$	$\gamma_4(T_k)$
3	−0.6627	1.8136	0.6777	0.276	0.024 72	0.9165	0.5572	−0.3206
4	−0.7882	2.1089	0.6261	0.237	0.012 66	0.9502	0.3752	−0.3947
5	−0.8969	2.3647	0.5979	0.211	0.007 48	0.9670	0.2746	−0.3803
6	−0.9940	2.5941	0.5801	0.193	0.004 85	0.9765	0.2119	−0.3478
7	−1.0827	2.8042	0.5678	0.178	0.003 35	0.9825	0.1697	−0.3142
8	−1.1647	2.9992	0.5588	0.167	0.002 43	0.9864	0.1398	−0.2837
9	−1.2413	3.1820	0.5519	0.157	0.001 82	0.9892	0.1176	−0.2572
10	−1.3135	3.3548	0.5465	0.149	0.001 41	0.9912	0.1007	−0.2344
11	−1.3820	3.5189	0.5421	0.142	0.001 12	0.9927	0.0874	−0.2147
12	−1.4473	3.6757	0.5384	0.136	0.000 90	0.9938	0.0768	−0.1978
13	−1.5097	3.8260	0.5354	0.131	0.000 74	0.9947	0.0681	−0.1831
14	−1.5697	3.9705	0.5327	0.126	0.000 62	0.9955	0.0610	−0.1703
15	−1.6275	4.1100	0.5305	0.122	0.000 52	0.9960	0.0550	−0.1591

Table 17.4 Optimal couples (λ^*, K^*) and optimal ARL^* for the EWMA-S^2 control chart, for $\tau \in \{0.6, 0.7, 0.8, 0.9, 0.95, 1.05, 1.1, 1.2, \ldots, 2\}$, $n \in \{3, 5, 7, 9\}$ and $ARL_0 = 370.4$

EWMA-S^2																
τ	$n=3$				$n=5$				$n=7$				$n=9$			
	λ^*	K^*	ARL^*	S^2	λ^*	K^*	ARL^*	S^2	λ^*	K^*	ARL^*	S^2	λ^*	K^*	ARL^*	S^2
0.60	0.10	2.690	17.8	267.0	0.17	2.782	9.0	102.2	0.25	2.836	6.2	45.6	0.31	2.863	4.7	23.6
0.70	0.08	2.644	28.5	363.1	0.12	2.724	14.6	184.5	0.17	2.791	10.0	102.5	0.20	2.823	7.7	62.3
0.80	0.05	2.547	54.3	467.0	0.08	2.635	28.2	308.2	0.10	2.689	19.5	211.8	0.12	2.733	15.1	152.5
0.90	0.05	2.547	155.8	512.1	0.05	2.515	81.0	445.8	0.05	2.505	56.8	384.1	0.06	2.556	44.7	333.1
0.95	0.05	2.547	325.7	463.7	0.05	2.515	202.9	451.0	0.05	2.505	150.6	433.1	0.05	2.501	120.9	414.7
1.05	0.05	2.547	153.6	268.8	0.05	2.515	121.4	253.5	0.05	2.505	99.3	242.1	0.05	2.501	84.0	232.3
1.10	0.05	2.547	64.9	186.4	0.05	2.515	44.8	159.6	0.05	2.505	34.9	140.8	0.05	2.501	29.0	126.2
1.20	0.05	2.547	21.6	90.1	0.05	2.515	15.3	64.5	0.05	2.505	12.4	50.0	0.05	2.501	10.7	40.5
1.30	0.05	2.547	11.6	48.0	0.05	2.515	8.8	30.5	0.05	2.505	7.4	22.0	0.05	2.501	6.6	16.9
1.40	0.05	2.547	7.8	28.5	0.05	2.515	6.2	16.8	0.05	2.505	5.3	11.7	0.30	2.861	4.7	8.8
1.50	0.05	2.547	5.9	18.6	0.05	2.515	4.8	10.5	0.42	2.848	4.2	7.2	0.46	2.864	3.4	5.4
1.60	0.05	2.547	4.8	13.1	0.05	2.515	4.0	7.2	0.49	2.839	3.2	4.9	0.54	2.854	2.7	3.7
1.70	0.05	2.547	4.0	9.8	0.05	2.515	3.5	5.3	0.57	2.827	2.6	3.6	0.65	2.836	2.2	2.8
1.80	0.05	2.547	3.5	7.7	0.55	2.830	2.9	4.2	0.66	2.811	2.2	2.9	0.73	2.822	1.9	2.2
1.90	0.05	2.547	3.1	6.2	0.55	2.830	2.5	3.4	0.66	2.811	2.0	2.4	0.77	2.815	1.6	1.9
2.00	0.05	2.547	2.9	5.2	0.63	2.829	2.3	2.9	0.74	2.799	1.8	2.0	0.78	2.813	1.5	1.6

is equal to

$$f_T(t) = \frac{1}{B_{S^2}(n)} \exp\left(\frac{t - A_{S^2}(n)}{B_{S^2}(n)}\right) \times f_{S^2}\left[\exp\left(\frac{t - A_{S^2}(n)}{B_{S^2}(n)}\right) - C_{S^2}(n)|n\right].$$

The fact that the distribution $f_T(t)$ of T_k depends only on n is important since it allows the calculation of the values of $E(T_k)$ and $\sigma(T_k)$ independently of the value of σ_0. The computation of $E(T_k)$ and $\sigma(T_k)$ has been achieved by numerical quadrature for $n \in \{3, \ldots, 15\}$, and the results are also shown in Table 17.3. Due to the fact that $E(T_k)$ approximates 0, whatever the sample size n, setting $E(T_k) = 0$ does not introduce significant errors into the statistical model. Finally, it seems logical to define the first value $Y_0 = E[a_{S^2} + b_{S^2} \ln(S^2 + c_{S^2})]$.

Using the first-order expansion of the expectation, we deduce $Y_0 \simeq a_{S^2} + b_{S^2} \ln(\sigma_0^2 + c_{S^2})$. Then by replacing a_{S^2}, b_{S^2} and c_{S^2} with $A_{S^2}(n) - 2B_{S^2}(n)\ln(\sigma_0)$, $B_{S^2}(n)$ and $C_{S^2}(n)\sigma_0^2$, we have

$$\begin{aligned} Y_0 \simeq\ & A_{S^2}(n) - 2B_{S^2}(n)\ln(\sigma_0) \\ & + B_{S^2}(n)\ln[\sigma_0^2 + C_{S^2}(n)\sigma_0^2] . \end{aligned}$$

After simplifications, we obtain:

$$Y_0 \simeq A_{S^2}(n) + B_{S^2}(n)\ln[1 + C_{S^2}(n)] .$$

As can be noticed, this value depends only on n and not on σ_0. The values for Y_0 are given in Table 17.3. One can note that these values are also close to 0 and can be replaced by 0 in practice with little practical effect.

Example 17.3: The goal of this example is to show how the EWMA-S^2 control chart behaves in the case of an increase and a decrease in the nominal process variability. The first 100 data points plotted in Fig. 17.5 (top and bottom) consist of 20 identical subgroups of $n = 5$ observations randomly generated from a normal $(20, 0.1)$ distribution (corresponding to an in-control process), while the last 50 data points of Fig. 17.5 (top) consist of 10 subgroups of $n = 5$ observations randomly generated from a normal $(20, 0.2)$ distribution (the nominal process standard deviation σ_0 has increased by a factor of 2), and the last 50 data points of Fig. 17.5 (bottom) consist of 10 subgroups of $n = 5$ observations randomly generated from a normal $(20, 0.05)$ distribution (the nominal process standard deviation σ_0 has decreased by a factor of 2). The corresponding 30 sample variances are plotted in Fig. 17.6, for the two cases (increasing and

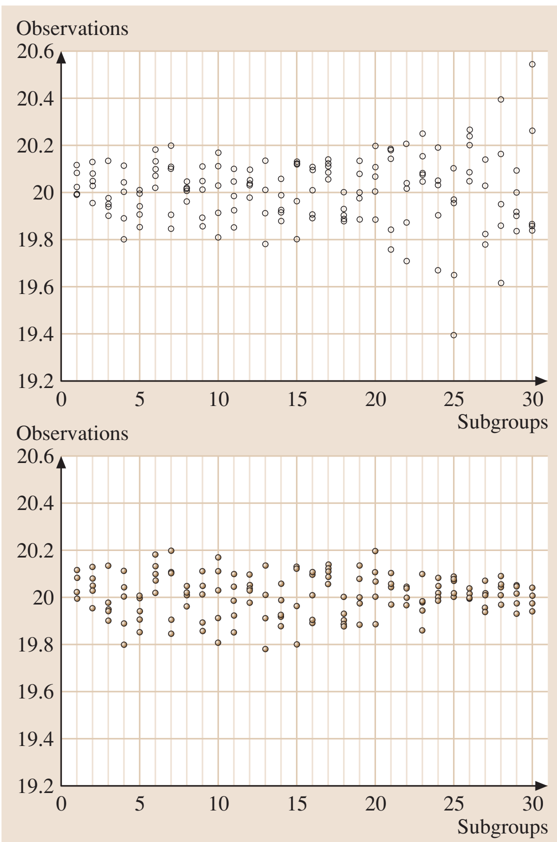

Fig. 17.5 Data with an increasing variance (*top*), and with a decreasing variance (*bottom*)

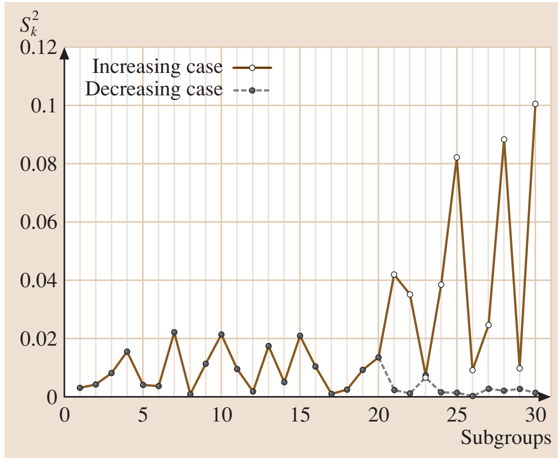

Fig. 17.6 Sample variances S_k^2 corresponding to the data of Fig. 17.5

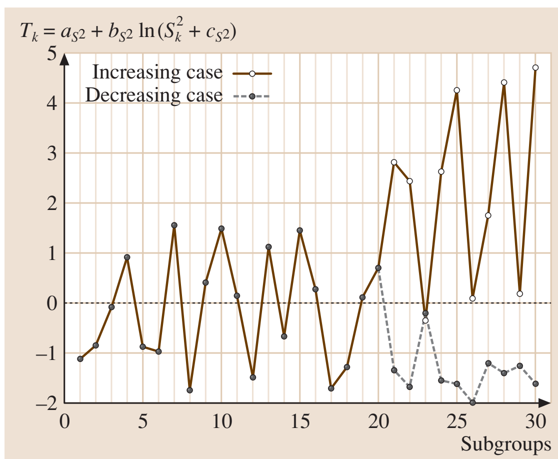

Fig. 17.7 Transformed sample variances $T_k = a_{S^2} + b_{S^2}\ln(S_k^2 + c_{S^2})$ corresponding to the data of Fig. 17.5

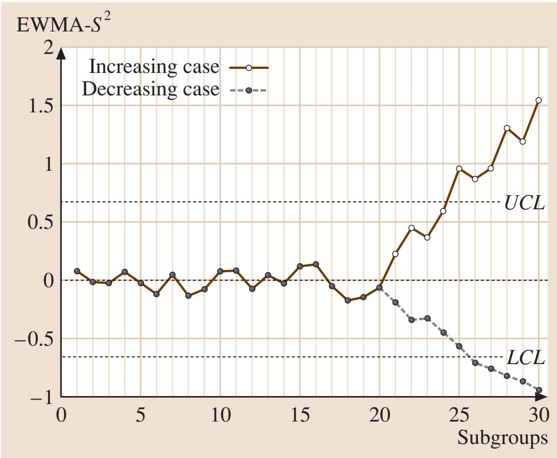

Fig. 17.8 EWMA-S^2 control chart ($\lambda = 0.1$, $K = 3$) corresponding to the data of Fig. 17.5

decreasing). At this step, the asymmetry between increasing and decreasing sample variances is particularly noticeable. If $n = 5$ and $\sigma_0 = 0.1$, then $b_{S^2} = 2.3647$, $c_{S^2} = 0.5979 \times 0.1^2 = 0.005\,979$ and $a_{S^2} = -0.8969 - 2 \times 2.3647 \times \ln(0.1) = 9.9929$. The 30 transformed sample variances are plotted in Fig. 17.7 and the EWMA-S^2 sequence along with the EWMA-S^2 control limits $LCL = 0.0075 - 3\sqrt{0.1/1.9} \times 0.967 = -0.658$ and $UCL = 0.0075 + 3\sqrt{0.1/1.9} \times 0.967 = 0.673$ ($\lambda = 0.1$ and $K = 3$) are plotted in Fig. 17.8. The EWMA-S^2 control chart clearly detects an out-of-control signal at the 25-th subgroup (in the increasing case) and at the 26-th subgroup (in the decreasing case), pointing out that an increase/decrease of the process variability occurred.

The distribution $f_T(t)$ of $T_k = a_{S^2} + b_{S^2} \ln(S_k^2 + c_{S^2})$ (plain line) for $n \in \{3, 5, 7, 9\}$, and the normal (0, 1) distribution (dotted line) are plotted in Fig. 17.9. The distribution of T_k is defined for $t \geq A_{S^2}(n) + B_{S^2}(n) \ln[C_{S^2}(n)]$, while the normal (0, 1) distribution is defined on $]-\infty, +\infty[$. This difference is particularly important for $n = 3$. It is clear that when n increases, the distribution of T_k becomes closer to the normal (0, 1) distribution, and the lower bound $A_{S^2}(n) + B_{S^2}(n) \ln[C_{S^2}(n)] \to -\infty$. By numerical quadrature, the skewness coefficient $\gamma_3(T_k) = \mu_3(T_k)/V^{3/2}(T_k)$ and the kurtosis coefficient $\gamma_4(T_k) = \mu_4(T_k)/V^2(T_k) - 3$ of T_k have been computed for $n = 3, \ldots, 15$. The results are shown in Table 17.3. As expected, when n increases, T_k becomes more normally distributed, i. e., $\gamma_3(T_k) \to 0$ and $\gamma_4(T_k) \to 0$.

Let σ_1 be the new out-of-control process standard deviation and let $\tau = \sigma_1/\sigma_0$ be the variable reflecting the shift in the process variability. Let $S_k'^2 = \sigma_1^2 S^2$ be the sample variance of n independent normal (μ_0, σ_1) random variables (i. e. the sample variance after a shift τ), and let $T_k' = a_{S^2} + b_{S^2} \ln(S_k'^2 + c_{S^2})$. If a_{S^2}, b_{S^2}, c_{S^2} and $S_k'^2$ are respectively replaced by $A_{S^2}(n) - 2B_{S^2}(n) \ln(\sigma_0)$, $B_{S^2}(n)$, $\sigma_0 C_{S^2}(n)$ and $\sigma_1^2 S^2$, then

$$\begin{aligned} T_k' &= A_{S^2}(n) - 2B_{S^2}(n) \ln(\sigma_0) \\ &\quad + B_{S^2}(n) \ln\left[\sigma_1^2 S^2 + \sigma_0^2 C_{S^2}(n)\right] \\ &= A_{S^2}(n) - 2B_{S^2}(n) \ln(\sigma_0) \\ &\quad + B_{S^2}(n) \ln\left\{\sigma_0^2[\tau^2 S^2 + C_{S^2}(n)]\right\} \\ &= A_{S^2}(n) + B_{S^2}(n) \ln[\tau^2 S^2 + C_{S^2}(n)]\,. \end{aligned}$$

This result clearly shows that the distribution $f_{T'}(t)$ of T_k' is equal to the distribution of the transformed random variable $\tau^2 S^2$. Consequently the p.d.f and the c.d.f of T_k' are

$$\begin{aligned} f_{T'}(t) &= \frac{1}{\tau^2 B_{S^2}(n)} \exp\left(\frac{t - A_{S^2}(n)}{B_{S^2}(n)}\right) \\ &\quad \times f_{S^2}\left\{\frac{1}{\tau^2}\left[\exp\left(\frac{t - A_{S^2}(n)}{B_{S^2}(n)}\right) - C_{S^2}(n)\right] \middle| n\right\}, \\ F_{T'}(t) &= F_{S^2}\left\{\frac{1}{\tau^2}\left[\exp\left(\frac{t - A_{S^2}(n)}{B_{S^2}(n)}\right) - C_{S^2}(n)\right] \middle| n\right\}. \end{aligned}$$

The ARL of the EWMA-S^2 control chart can be computed using one of the methods presented in Sect. 17.1.3. Like for the EWMA-$\bar{X}$ and EWMA-$\tilde{X}$ control charts, it is sometimes interesting for the quality practitioner to know the optimal couples (λ^*, K^*) that give the same in-control $ARL_Y = ARL_0$ (i. e. the ARL when the process is functioning at the nominal variability $\sigma = \sigma_0$ or equivalently $\tau = 1$) and then find, for a specified value of the shift τ, the unique couple (λ^*, K^*) which yields the smallest possible out-of-control $ARL_Y = ARL^*$. In order to compute the couples (λ^*, K^*) for the EWMA-S^2 control chart, the same approach as in the EWMA-$\bar{X}$ and EWMA-$\tilde{X}$ control charts was adopted:

1. For every $\lambda \in \{0.05, 0.06, \ldots, 1\}$ and for $\tau = 1$, we computed the corresponding value K such that $ARL_Y = ARL_0$. At the end of this step, we have a set of pairs $\{(0.05, K_{0.05}), (0.06, K_{0.06}), \ldots, (1, K_1)\}$ candidating for the second step.
2. For every shift $\tau \in \{0.6, 0.7, 0.8, 0.9, 0.95, 1.05, 1.1, 1.2, \ldots, 2\}$, and for every pair $\{(0.05, K_{0.05}), (0.06, K_{0.06}), \ldots, (1, K_1)\}$ we computed ARL_Y and chose the pair (λ^*, K^*) which gave the minimum $ARL_Y = ARL_Y^*$.

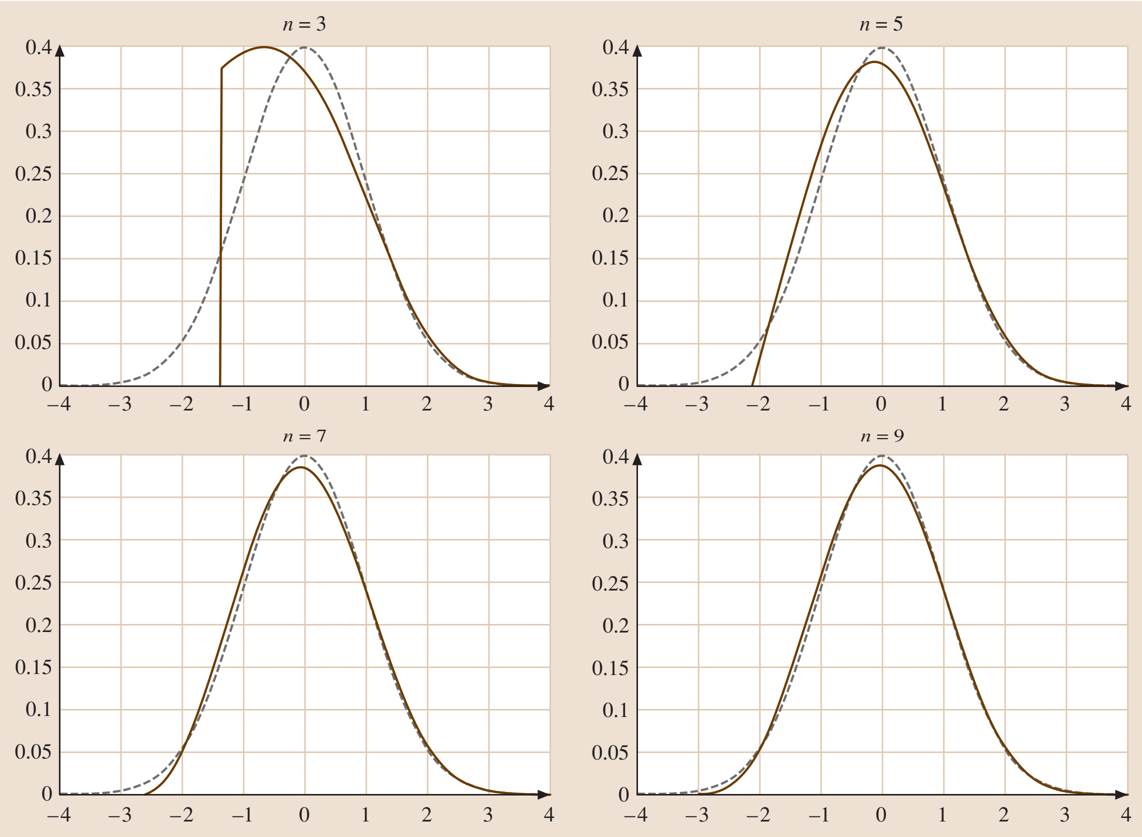

Fig. 17.9 Distribution $f_T(t)$ of $T_k = a_{S^2} + b_{S^2} \ln(S_k^2 + c_{S^2})$ (*plain line*) compared with the normal (0, 1) distribution (*dotted line*), for $n \in \{3, 5, 7, 9\}$

The optimal couples (λ^*, K^*) for the EWMA-S^2 control chart and the corresponding minimal ARL^* are shown in Table 17.4. In Table 17.4, we also added, for comparison purpose, the ARL of the classic S^2 control chart. For example, the optimal couple (λ^*, K^*) ensuring the smallest ARL for a shift $\tau = 1.2$ and $n = 7$ is (0.05, 2.505) and the corresponding minimal ARL is $ARL^* = 12.4$, while for the classic S^2 control chart, we have $ARL = 50.0$. This is just an example of the superiority of the EWMA-S^2 control chart (with optimized parameters) over the classical S^2 control chart when the shift τ is small.

17.3.2 EWMA-*S* Control Chart

The EWMA-S control chart proposed by *Castagliola* [17.26] is a natural extension of the EWMA-S^2 control chart where a three-parameter (a_S, b_S, c_S) logarithmic transformation is applied to the sample standard deviation S_k, [i. e. $T_k = a_S + b_S \ln(S_k + c_S)$], instead of the sample variance S_k^2. The control limits of the EWMA-S control chart are given by (17.4) and (17.5) but with different values for $E(T_k)$ and $\sigma(T_k)$. The p.d.f. and the c.d.f. of S are defined for $s \geq 0$ and are equal to

$$f_S(s) = 2s f_\gamma \left(s^2 | \frac{n-1}{2}, \frac{2}{n-1} \right) ,$$

$$F_S(s) = F_\gamma \left(s^2 | \frac{n-1}{2}, \frac{2}{n-1} \right) ,$$

and the mean $E(S)$, the variance $V(S)$, and the skewness coefficient $\gamma_3(S)$ of S are equal to

$$E(S) = K_S(n, 1) ,$$

$$V(S) = 1 - K_S^2(n, 1) ,$$

Table 17.5 Constants $A_S(n)$, $B_S(n)$, $C_S(n)$, Y_0, $E(T_k)$, $\sigma(T_k)$, $\gamma_3(T_k)$ and $\gamma_4(T_k)$ for the EWMA-S control chart, for $n \in \{3, \dots, 15\}$

EWMA-S								
n	$A_S(n)$	$B_S(n)$	$C_S(n)$	Y_0	$E(T_k)$	$\sigma(T_k)$	$\gamma_3(T_k)$	$\gamma_4(T_k)$
3	−3.8134	4.8729	1.3474	0.1026	0.000 92	0.9917	0.1361	−0.4489
4	−5.4669	6.2696	1.5009	0.0797	0.000 30	0.9965	0.0741	−0.3221
5	−6.8941	7.4727	1.5984	0.0669	0.000 14	0.9981	0.0472	−0.2454
6	−8.1528	8.5370	1.6650	0.0586	0.000 07	0.9988	0.0331	−0.1964
7	−9.2839	9.4980	1.7131	0.0526	0.000 04	0.9992	0.0248	−0.1628
8	−10.3158	10.3789	1.7493	0.0482	0.000 03	0.9994	0.0194	−0.1387
9	−11.2684	11.1958	1.7776	0.0447	0.000 02	0.9996	0.0157	−0.1206
10	−12.1562	11.9605	1.8002	0.0418	0.000 01	0.9997	0.0130	−0.1066
11	−12.9901	12.6813	1.8186	0.0394	0.000 01	0.9997	0.0110	−0.0955
12	−13.7783	13.3650	1.8340	0.0374	0.000 01	0.9998	0.0095	−0.0864
13	−14.5272	14.0164	1.8469	0.0357	0.000 01	0.9998	0.0082	−0.0789
14	−15.2418	14.6397	1.8581	0.0342	0.000 01	0.9998	0.0073	−0.0725
15	−15.9264	15.2382	1.8677	0.0328	0.000 00	0.9999	0.0065	−0.0671

$$\gamma_3(S) = \frac{K_S(n,3) - 3K_S(n,1) + 2K_S^3(n,1)}{[1 - K_S^2(n,1)]^{3/2}} ,$$

where

$$K_S(n,r) = \frac{\Gamma[(n-1+r)/2]}{\Gamma[(n-1)/2]} \left(\frac{2}{n-1}\right)^{r/2} .$$

Using similar demonstrations as for the EWMA-S^2 control chart, it can be proven that the constants a_S, b_S and c_S required for the transformation $T_k = a_S + b_S \ln(S_k + c_S)$ can be deduced from the constants $A_S(n)$, $B_S(n)$ and $C_S(n)$ using the following relations

$$b_S = B_S(n) ,$$
$$c_S = C_S(n)\sigma_0 ,$$
$$a_S = A_S(n) - B_S(n)\ln(\sigma_0) .$$

It can also be proven that the initial value Y_0 is equal to

$$Y_0 = A_S(n) + B_S(n)\ln[K_S(n,1) + C_S(n)] .$$

All the constants $A_S(n)$, $B_S(n)$, $C_S(n)$, Y_0, $E(T_k)$ and $\sigma(T_k)$, useful for the EWMA-S control chart, are shown in Table 17.5 for $n \in \{3, \dots, 15\}$.

Example 17.4: The goal of this example is to show how the EWMA-S control chart behaves in the case of an increase and a decrease in the nominal process variability. We reuse the data in Fig. 17.5 (top and bottom). The corresponding 30 sample standard deviations are plotted in Fig. 17.10, for the two cases (increasing and decreasing). If $n = 5$ and $\sigma_0 = 0.1$, then $b_S = 7.4727$, $c_S = 1.5984 \times 0.1 = 0.159\,84$ and $a_S = -6.8941 - 7.4727 \times \ln(0.1) = 10.3124$. The 30 transformed sample standard deviations are plotted in Fig. 17.11 and the EWMA-S sequence along with the EWMA-S control limits $LCL = 0.000\,14 - 3\sqrt{0.1/1.9} \times 0.9981 = -0.687$ and $UCL = 0.000\,14 + 3\sqrt{0.1/1.9} \times 0.9981 = 0.687$ ($\lambda = 0.1$ and $K = 3$) are plotted in Fig. 17.12. The EWMA-S control chart clearly detects an out-of-control signal at the 25-th subgroup (in the increasing case) and at the 26-th subgroup (in the decreasing case), pointing out that an increase/decrease of the standard deviation occurred.

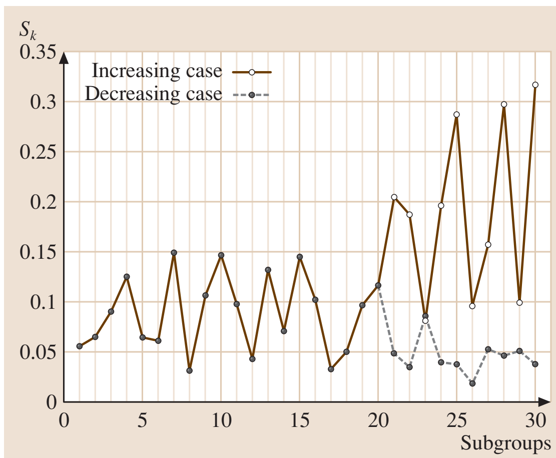

Fig. 17.10 Sample standard deviations S_k corresponding to the data of Fig. 17.5

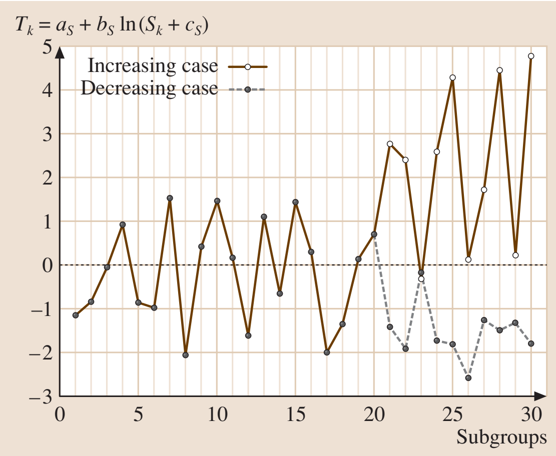

Fig. 17.11 Transformed standard deviations $T_k = a_S + b_S \ln(S_k + c_S)$ corresponding to the data of Fig. 17.5

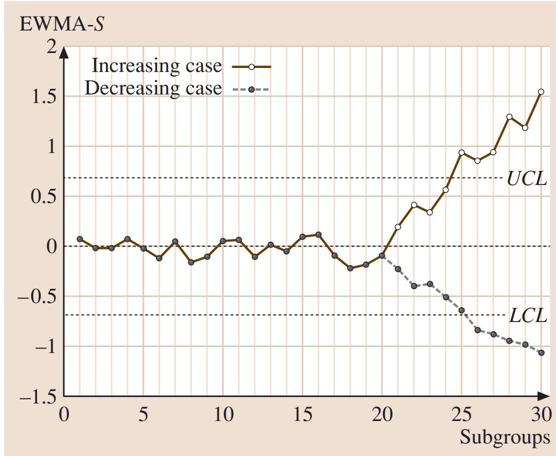

Fig. 17.12 EWMA-S control chart ($\lambda = 0.1$, $K = 3$) corresponding to the data of Fig. 17.5

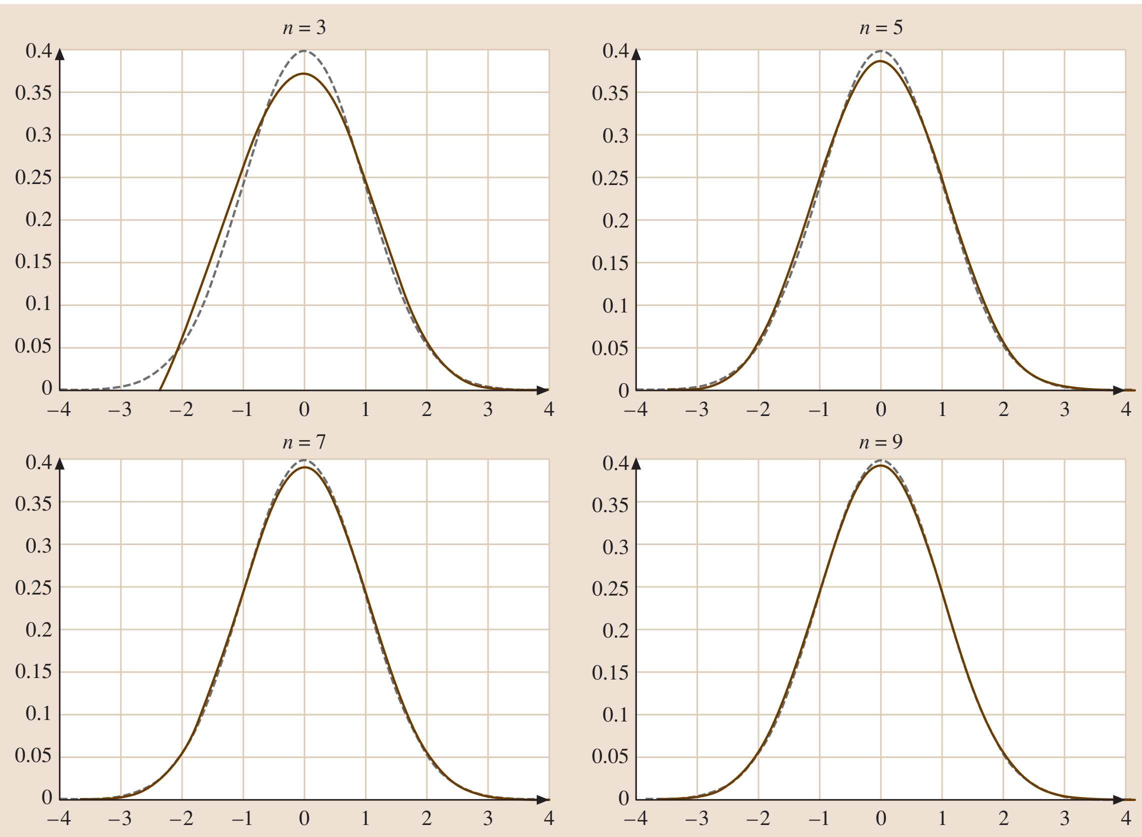

Fig. 17.13 Distribution $f_T(t)$ of $T_k = a_S + b_S \ln(S_k + c_S)$ (*plain line*) compared with the normal (0, 1) distribution (*dotted* line), for $n \in \{3, 5, 7, 9\}$

Table 17.6 Optimal couples (λ^*, K^*) and optimal ARL^* for the EWMA-S control chart, for $\tau \in \{0.6, 0.7, 0.8, 0.9, 0.95, 1.05, 1.1, 1.2, \ldots, 2\}$, $n \in \{3, 5, 7, 9\}$ and $ARL_0 = 370.4$

EWMA-S																
τ	$n=3$				$n=5$				$n=7$				$n=9$			
	λ^*	K^*	ARL^*	S	λ^*	K^*	ARL^*	S	λ^*	K^*	ARL^*	S	λ^*	K^*	ARL^*	S
0.60	0.10	2.680	14.9	267.0	0.17	2.800	7.9	102.2	0.25	2.867	5.6	45.6	0.29	2.892	4.4	23.6
0.70	0.07	2.590	24.3	363.1	0.12	2.732	13.0	184.5	0.14	2.772	9.1	102.5	0.19	2.834	7.2	62.3
0.80	0.05	2.491	46.2	467.0	0.07	2.594	25.0	308.2	0.08	2.635	17.7	211.8	0.11	2.720	13.9	152.5
0.90	0.05	2.491	132.9	512.1	0.05	2.490	72.2	445.8	0.05	2.490	51.0	384.1	0.05	2.490	40.1	333.1
0.95	0.05	2.491	273.7	463.7	0.05	2.490	183.7	451.0	0.05	2.490	139.2	433.1	0.05	2.490	112.5	414.7
1.05	0.05	2.491	197.7	268.8	0.05	2.490	145.6	253.5	0.05	2.490	115.2	242.1	0.05	2.490	95.8	232.3
1.10	0.05	2.491	94.4	186.4	0.05	2.490	58.8	159.6	0.05	2.490	43.7	140.8	0.05	2.490	35.5	126.2
1.20	0.05	2.491	35.7	90.1	0.05	2.490	22.0	64.5	0.05	2.490	16.7	50.0	0.10	2.696	13.6	40.5
1.30	0.05	2.491	20.4	48.0	0.11	2.713	12.8	30.5	0.17	2.809	9.5	22.0	0.18	2.824	7.7	16.9
1.40	0.05	2.491	14.2	28.5	0.20	2.824	8.6	16.8	0.24	2.862	6.3	11.7	0.32	2.902	5.1	8.8
1.50	0.20	2.793	10.6	18.6	0.32	2.868	6.3	10.5	0.34	2.894	4.6	7.2	0.41	2.918	3.7	5.4
1.60	0.43	2.791	8.1	13.1	0.43	2.870	4.8	7.2	0.49	2.903	3.6	4.9	0.55	2.922	2.9	3.7
1.70	0.56	2.753	6.4	9.8	0.51	2.861	3.9	5.3	0.53	2.901	2.9	3.6	0.63	2.919	2.4	2.8
1.80	0.62	2.734	5.3	7.7	0.60	2.846	3.2	4.2	0.64	2.892	2.4	2.9	0.69	2.916	2.0	2.2
1.90	0.65	2.725	4.5	6.2	0.66	2.835	2.8	3.4	0.70	2.886	2.1	2.4	0.74	2.913	1.7	1.9
2.00	0.67	2.720	3.9	5.2	0.70	2.827	2.4	2.9	0.74	2.882	1.9	2.0	0.74	2.913	1.6	1.6

The distribution $f_T(t)$ of $T_k = a_S + b_S \ln(S_k + c_S)$ (plain line) for $n \in \{3, 5, 7, 9\}$, and the normal $(0, 1)$ distribution (dotted line) are plotted in Fig. 17.13. It is clear that, when n increases, the distribution of T_k becomes closer to the normal $(0, 1)$ distribution, and the lower bound $A_S(n) + B_S(n) \ln[C_S(n)] \to -\infty$. By numerical quadrature, the skewness coefficient $\gamma_3(T_k)$ and the kurtosis coefficient $\gamma_4(T_k)$ of T_k have been computed for $n \in \{3, \ldots, 15\}$; see Table 17.5. As expected, when n increases, T_k becomes more normally distributed, i. e., $\gamma_3(T_k) \to 0$ and $\gamma_4(T_k) \to 0$.

The p.d.f and the c.d.f of the transformed sample standard deviation $T'_k = a_S + b_S \ln(S'_k + c_S)$ after a shift τ are equal to

$$\begin{aligned} f_{T'}(t) &= \frac{1}{\tau B_S(n)} \exp\left(\frac{t - A_S(n)}{B_S(n)}\right) \\ &\quad \times f_S\left\{\frac{1}{\tau}\left[\exp\left(\frac{t - A_S(n)}{B_S(n)}\right) - C_S(n)\right] \middle| n\right\} , \\ F_{T'}(t) &= F_S\left\{\frac{1}{\tau}\left[\exp\left(\frac{t - A_S(n)}{B_S(n)}\right) - C_S(n)\right] \middle| n\right\} . \end{aligned}$$

The ARL of the EWMA-S control chart can be computed using one of the methods presented in Sect. 17.2.3. The method used for computing the optimal couples (λ^*, K^*) and the corresponding minimal ARL^* for the EWMA-S control chart is exactly the same as the one used for the EWMA-S^2 control chart. The results are shown in Table 17.6. In Table 17.6, we also added, for comparison purpose, the ARL of the classical S control chart. For example, the optimal couple (λ^*, K^*) ensuring the smallest ARL for a shift $\tau = 1.2$ and $n = 7$ is $(0.05, 2.490)$ and the corresponding minimal ARL is $ARL^* = 16.7$, while for the classic S control chart, we have $ARL = 50.0$. Like the EWMA-S^2 control chart, the EWMA-S control chart (with optimized parameters) is more efficient, in terms of ARL, than the S^2 or S control chart. The results of both EWMA-S^2 and EWMA-S control chart are very similar. The main difference is that for the decreasing case $(\tau < 1)$ the optimal ARL^*s of the EWMA-S control chart are smaller than those of the EWMA-S^2 control chart, while for the increasing case $(\tau > 1)$ the opposite results.

17.3.3 EWMA-*R* Control Chart

Let R_k be the range of the subgroup k, i. e.,

$$R_k = \max(X_{k,1}, \ldots, X_{k,n}) - \min(X_{k,1}, \ldots, X_{k,n}) .$$

The EWMA-R control chart proposed by *Castagliola* [17.27] is a natural extension of the EWMA-S^2 control chart where a three-parameter (a_R, b_R, c_R) logarithmic transformation is applied to the range R_k, [i. e. $T_k = a_R + b_R \ln(R_k + c_R)$], instead of the sample vari-

Table 17.7 Expectation $E(R)$, variance $V(R)$ and skewness coefficient $\gamma_3(R)$ of R

n	$E(R)$	$V(R)$	$\gamma_3(R)$
3	1.6926	0.7892	0.6461
4	2.0588	0.7741	0.5230
5	2.3259	0.7466	0.4655
6	2.5344	0.7192	0.4350
7	2.7044	0.6942	0.4176
8	2.8472	0.6721	0.4073
9	2.9700	0.6526	0.4011
10	3.0775	0.6353	0.3976
11	3.1729	0.6199	0.3957
12	3.2585	0.6060	0.3949
13	3.3360	0.5935	0.3949
14	3.4068	0.5822	0.3953
15	3.4718	0.5719	0.3961

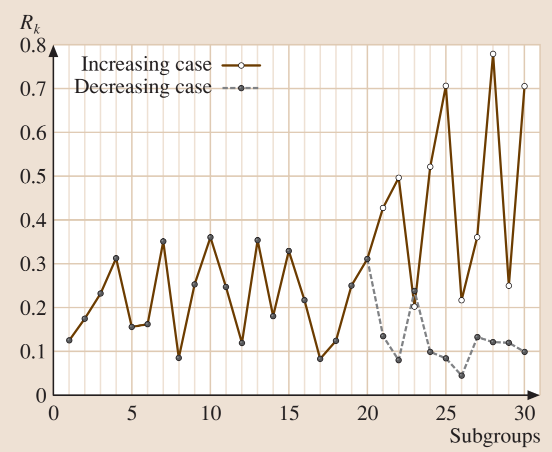

Fig. 17.14 Sample ranges R_k corresponding to the data of Fig. 17.5

ance S_k^2. The control limits of the EWMA-R control chart are given by (17.4) and (17.5) but with different values for $E(T_k)$ and $\sigma(T_k)$. Let R be the range of n independent normal $(\mu_0, 1)$ random variables. The p.d.f. $f_R(r)$ of R is defined for $r \geq 0$ and is given by the well-known relation

$$f_R(r) = n(n-1) \int_{-\infty}^{+\infty} \phi(u)\phi(r+u)[\Phi(r+u) - \Phi(u)]^{n-2}\,\mathrm{d}u \,.$$

In order to compute the constants $A_R(n)$, $B_R(n)$ and $C_R(n)$, the expectation $E(R)$, the variance $V(R)$ and the skewness coefficient $\gamma_3(R)$ of R have been computed by numerical quadrature and are tabulated in Table 17.7. Using similar demonstrations as for the EWMA-S control chart, it can be proven that the constants a_R, b_R and c_R required for the transformation $T_k = a_R + b_R \ln(R_k + c_R)$ can be deduced from the constants $A_R(n)$, $B_R(n)$ and $C_R(n)$ using the following relations

$$b_R = B_R(n)\,,$$
$$c_R = C_R(n)\sigma_0\,,$$

Table 17.8 Constants $A_R(n)$, $B_R(n)$, $C_R(n)$, Y_0, $E(T_k)$, $\sigma(T_k)$, $\gamma_3(T_k)$ and $\gamma_4(T_k)$ for the EWMA-R control chart, for $n \in \{3, \ldots, 15\}$

EWMA-R								
n	$A_R(n)$	$B_R(n)$	$C_R(n)$	Y_0	$E(T_k)$	$\sigma(T_k)$	$\gamma_3(T_k)$	$\gamma_4(T_k)$
3	−6.7191	4.7655	2.4944	0.105	0.000 96	0.9915	0.1370	−0.4429
4	−9.4200	5.8364	3.0385	0.086	0.000 36	0.9961	0.0761	−0.3099
5	−11.1940	6.5336	3.2866	0.077	0.000 19	0.9977	0.0499	−0.2288
6	−12.3056	6.9804	3.3549	0.072	0.000 12	0.9985	0.0361	−0.1767
7	−12.9778	7.2649	3.3202	0.069	0.000 09	0.9989	0.0278	−0.1412
8	−13.3653	7.4446	3.2286	0.067	0.000 07	0.9991	0.0223	−0.1158
9	−13.5689	7.5559	3.1072	0.066	0.000 05	0.9993	0.0185	−0.0969
10	−13.6531	7.6220	2.9715	0.066	0.000 04	0.9994	0.0157	−0.0823
11	−13.6595	7.6576	2.8304	0.065	0.000 04	0.9995	0.0135	−0.0708
12	−13.6151	7.6726	2.6892	0.065	0.000 03	0.9995	0.0118	−0.0615
13	−13.5378	7.6736	2.5508	0.065	0.000 03	0.9996	0.0105	−0.0538
14	−13.4393	7.6647	2.4167	0.065	0.000 03	0.9996	0.0093	−0.0474
15	−13.3276	7.6492	2.2879	0.065	0.000 02	0.9997	0.0084	−0.0420

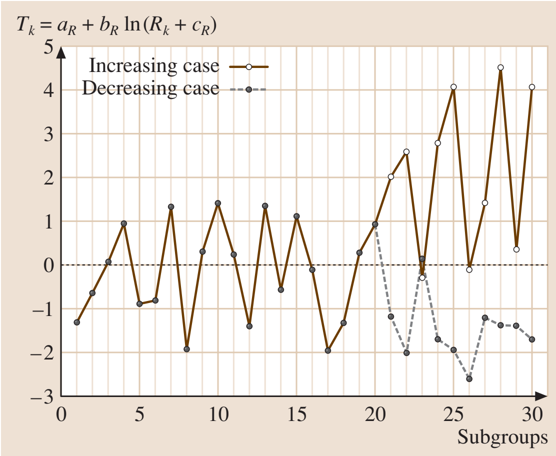

Fig. 17.15 Transformed ranges $T_k = a_R + b_R \ln(R_k + c_R)$ corresponding to the data of Fig. 17.5

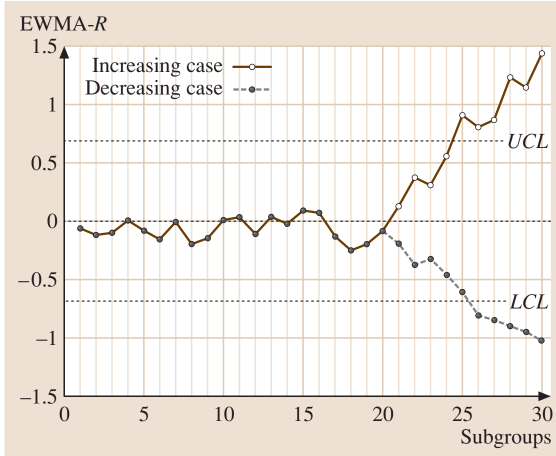

Fig. 17.16 EWMA-R control chart ($\lambda = 0.1$, $K = 3$) corresponding to the data of Fig. 17.5

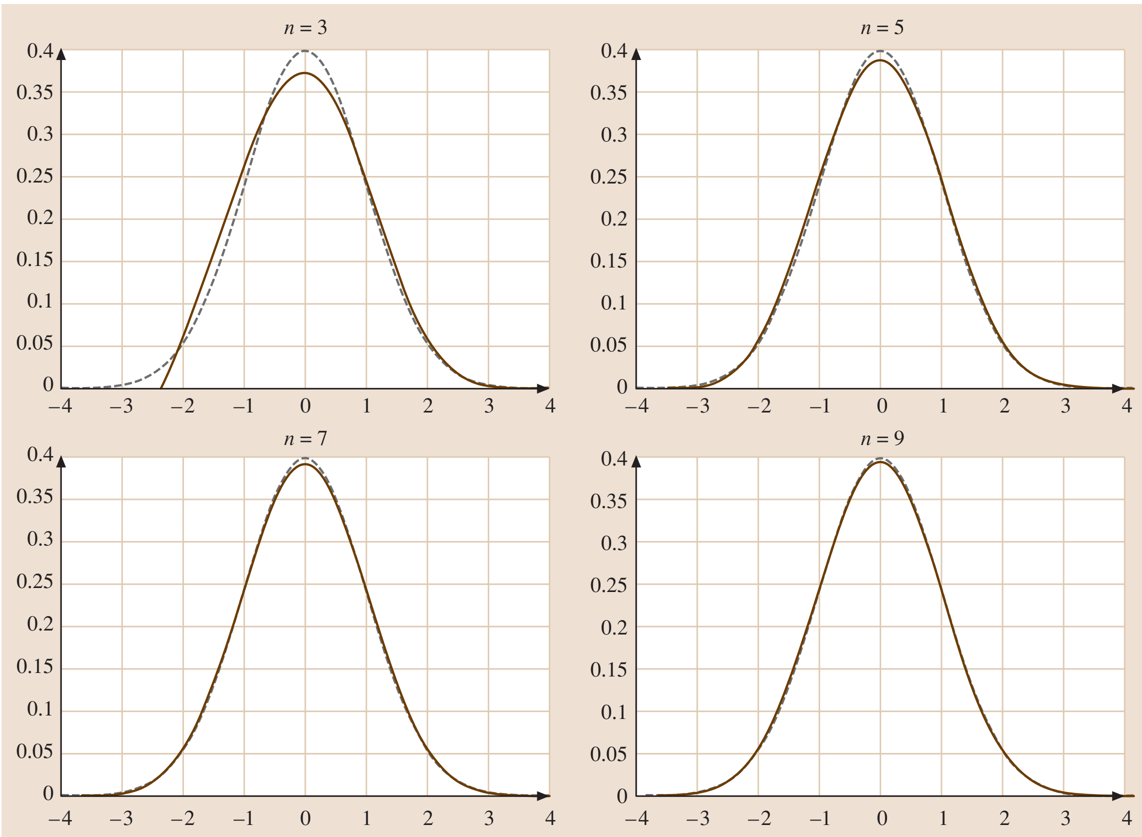

Fig. 17.17 Distribution $f_T(t)$ of $T_k = a_R + b_R \ln(R_k + c_R)$ (*plain line*) compared with the normal (0, 1) distribution (*dotted line*), for $n \in \{3, 5, 7, 9\}$

Table 17.9 Optimal couples (λ^*, K^*) and optimal ARL^* for the EWMA-R control chart, for $\tau \in \{0.6, 0.7, 0.8, 0.9, 0.95, 1.05, 1.1, 1.2, \dots, 2\}$, $n \in \{3, 5, 7, 9\}$ and $ARL_0 = 370.4$

EWMA-*R*																
τ	$n=3$				$n=5$				$n=7$				$n=9$			
	λ^*	K^*	ARL^*	R	λ^*	K^*	ARL^*	R	λ^*	K^*	ARL^*	R	λ^*	K^*	ARL^*	R
0.60	0.10	2.680	15.0	267.0	0.18	2.811	8.2	102.4	0.22	2.854	5.9	46.4	0.27	2.890	4.7	24.8
0.70	0.07	2.591	24.5	363.0	0.11	2.714	13.4	184.7	0.15	2.788	9.7	103.6	0.17	2.817	7.8	64.2
0.80	0.05	2.491	46.6	466.3	0.07	2.595	25.9	307.9	0.08	2.635	19.0	212.7	0.10	2.697	15.4	155.0
0.90	0.05	2.491	133.9	509.6	0.05	2.491	75.0	440.3	0.05	2.491	54.9	378.8	0.05	2.491	44.8	329.6
0.95	0.05	2.491	274.9	461.7	0.05	2.491	188.4	444.5	0.05	2.491	147.5	423.4	0.05	2.491	123.4	403.2
1.05	0.05	2.491	198.1	270.7	0.05	2.491	149.3	261.3	0.05	2.491	122.2	256.5	0.05	2.491	105.4	253.2
1.10	0.05	2.491	94.7	189.0	0.05	2.491	60.5	169.8	0.05	2.491	46.5	158.5	0.05	2.491	39.0	150.4
1.20	0.05	2.491	35.8	92.3	0.05	2.491	22.5	71.7	0.05	2.491	17.6	60.9	0.05	2.491	15.0	53.9
1.30	0.05	2.491	20.4	49.5	0.08	2.633	13.3	34.6	0.12	2.739	10.3	27.6	0.16	2.805	8.7	23.5
1.40	0.05	2.491	14.2	29.5	0.17	2.802	9.0	19.2	0.21	2.847	6.9	14.8	0.25	2.880	5.9	12.3
1.50	0.18	2.782	10.7	19.3	0.26	2.857	6.6	12.0	0.27	2.880	5.1	9.0	0.34	2.913	4.3	7.4
1.60	0.45	2.788	8.2	13.6	0.33	2.873	5.1	8.2	0.37	2.905	4.0	6.1	0.45	2.930	3.4	5.0
1.70	0.56	2.756	6.5	10.1	0.44	2.876	4.1	6.0	0.50	2.912	3.3	4.5	0.48	2.932	2.8	3.6
1.80	0.58	2.750	5.4	7.9	0.55	2.864	3.5	4.7	0.52	2.912	2.7	3.5	0.61	2.934	2.3	2.8
1.90	0.64	2.732	4.6	6.4	0.61	2.854	3.0	3.8	0.63	2.905	2.4	2.8	0.67	2.932	2.0	2.3
2.00	0.67	2.724	4.0	5.3	0.63	2.850	2.6	3.2	0.68	2.901	2.1	2.4	0.71	2.930	1.8	2.0

$$a_R = A_R(n) - B_R(n)\ln(\sigma_0)\,.$$

It can also be proven that the initial value Y_0 is equal to

$$Y_0 = A_R(n) + B_R(n)\ln[K_R(n) + C_R(n)]\,,$$

where $K_R(n)$ is equal to

$$K_R(n) = 2\int_0^{+\infty} 1 - \left[\Phi(x)\right]^n - \left[1 - \Phi(x)\right]^n \,\mathrm{d}x\,.$$

All the constants $A_R(n)$, $B_R(n)$, $C_R(n)$, Y_0, $E(T_k)$ and $\sigma(T_k)$, useful for the EWMA-R control chart, are shown in Table 17.8 for $n \in \{3, \dots, 15\}$.

Example 17.5: The goal of this example is to show how the EWMA-R control chart behaves in the case of an increase and a decrease in the nominal variability. We reuse the data in Fig. 17.5 (top and bottom). The corresponding 30 sample ranges are plotted in Fig. 17.14, for the two cases (increasing and decreasing). If $n = 5$ and $\sigma_0 = 0.1$, then $b_R = 6.5336$, $c_R = 3.2866 \times 0.1 = 0.328\,66$ and $a_R = -11.1940 - 6.5336 \times \ln(0.1) = 3.8502$. The 30 transformed ranges are plotted in Fig. 17.15 and the EWMA-R sequence along with the EWMA-R control limits $LCL = 0.000\,19 - 3\sqrt{0.1/1.9} \times 0.9977 = -0.686$ and $UCL = 0.000\,19 + 3\sqrt{0.1/1.9} \times 0.9977 = 0.687$ ($\lambda = 0.1$ and $K = 3$) are plotted in Fig. 17.16. The EWMA-R control chart clearly detects an out-of-control signal at the 25-th subgroup (in the increasing case) and at the 26-th subgroup (in the decreasing case), pointing out that an increase/decrease of the dispersion occurred.

The distribution $f_T(t)$ of $T_k = a_R + b_R \ln(R_k + c_R)$ (plain line) for $n \in \{3, 5, 7, 9\}$, and the normal (0, 1) distribution (dotted line) are plotted in Fig. 17.17. It is clear that, when n increases, the distribution of T_k becomes closer to the normal (0, 1) distribution, and the lower bound $A_R(n) + B_R(n)\ln[C_R(n)] \to -\infty$. By numerical quadrature, the skewness coefficient $\gamma_3(T_k)$ and the kurtosis coefficient $\gamma_4(T_k)$ of T_k have been computed for $n \in \{3, \dots, 15\}$; see Table 17.8. As expected, when n increases, T_k becomes more normally distributed, i. e., $\gamma_3(T_k) \to 0$ and $\gamma_4(T_k) \to 0$.

The p.d.f and the c.d.f of the transformed range $T'_k = a_R + b_R \ln(R'_k + c_R)$ after a shift τ are equal to

$$f_{T'}(t) = \frac{1}{\tau B_R(n)} \exp\left(\frac{t - A_R(n)}{B_R(n)}\right) \times f_R\left\{\frac{1}{\tau}\left[\exp\left(\frac{t - A_R(n)}{B_R(n)}\right) - C_R(n)\right] \middle| n\right\}\,,$$

$$F_{T'}(t) = F_R\left\{\frac{1}{\tau}\left[\exp\left(\frac{t - A_R(n)}{B_R(n)}\right) - C_R(n)\right] \middle| n\right\}\,.$$

The *ARL* of the EWMA-R control chart can be computed using one of the methods presented in Sect. 17.2.3. The method used for computing the optimal couples (λ^*, K^*) and the corresponding minimal ARL^* for the EWMA-R control chart is exactly the same as the one used for the EWMA-S control chart. The results are shown in Table 17.9. In Table 17.9, we also added, for comparison purpose, the *ARL* of the classic R control chart. For example, the optimal couple (λ^*, K^*) ensuring the smallest *ARL* for a shift $\tau = 1.2$ and $n = 7$ is (0.05, 2.491) and the corresponding minimal *ARL* is $ARL^* = 17.6$, while for the classic R control chart, we have $ARL = 60.9$. The EWMA-R control chart (with optimized parameters) is more efficient, in terms of *ARL*, than the R control chart, but is slightly less efficient than both the EWMA-S^2 and EWMA-S control charts.

17.4 Variable Sampling Interval EWMA Control Charts for Process Dispersion

17.4.1 Introduction

Variable sampling intervals (VSI) control charts are a class of adaptive control charts whose sampling intervals are selected depending on what is observed from the process. VSI control charts have been demonstrated to detect process changes faster than fixed sampling interval (FSI) control charts.

For the VSI charts investigated here, the policy of sampling interval selection is dual: if a point falls into a warning zone near to one of the control limits, the sampling interval to the successive sample should be shorter; otherwise, if the last plotted point is plotted near to the central line, the successive sampling interval can be enlarged, because there is not doubt about a possible out-of-control condition. Most work on developing VSI control charts has been done for the problem of monitoring the mean of the process (see *Reynolds* et al. [17.28], *Reynolds* et al. [17.29], *Runger* and *Pignatiello* [17.30], *Saccucci* et al. [17.31] and *Reynolds* [17.32]). However, fewer works have been done on control charts for the process variance. *Chengular* et al. [17.33] considered a VSI Shewhart chart for monitoring process mean and variance, and very recently, *Reynolds* and *Stoumbos* [17.34] investigated a combination of different control charts for both process mean and variance, using individual observations and variable sampling intervals.

17.4.2 VSI Strategy

Unlike FSI control schemes, the sampling interval between T_k and T_{k+1} depends on the current value of Y_k. A longer sampling interval h_L is used when the control statistic falls within the region $R_L = [LWL, UWL]$, defined as

$$LWL = E(T_k) - W\sqrt{\frac{\lambda}{2-\lambda}}\sigma(T_k)\,,$$

$$UWL = E(T_k) + W\sqrt{\frac{\lambda}{2-\lambda}}\sigma(T_k)\,,$$

where W is the width of the *warning limits*, which are always inside the control interval, i.e., $W < K$. Similarly, a short sampling interval h_S is used when the control statistic falls within the region $R_S = [LCL, LWL] \cup [UWL, UCL]$. The process is considered out of control and action should be taken whenever Y_k falls outside the range of the control limits $[LCL, UCL]$. This dual-waiting-time control chart is known to be optimal and easy to implement in practice. *Reynolds* et al. [17.28] have empirically shown that it is optimal to use only two sampling intervals with VSI Shewhart and VSI cumulative sum (CUSUM) control scheme for detecting a specified shift in the process target values. They also gave a general proof for any control scheme that can be represented as a Markov chain. *Saccucci* et al. [17.31] gave a simplified proof based on the theory of Markov chain. In general, these optimality proofs show that the short sampling interval h_S should be made as short as possible, while the long sampling interval h_L should be made as long as possible (i. e. the longest amount of time that is reasonable for the process to run without sampling). As pointed out by *Lucas* and *Saccucci* [17.5], there are practical limitations on how short h_S should be. The value of h_S represents the shortest feasible time interval between subgroups from the process. Any shorter time between subgroups would be impossible due to the amount of time that is required to form the rational subgroups, carry out the inspection, analyze the results from any testing procedures, transport parts and materials, and other delays that would be otherwise inconvenient. So, in this paper we will consider the impact on the expected time until detection, using small but nonzero values of h_S.

Table 17.10 Optimal out-of-control ATS^* of the VSI EWMA-S^2 for $\tau \in \{0.6, 0.7, 0.8, 0.9, 0.95, 1.05, 1.1, 1.2, \dots, 2\}$, $n \in \{3, 5\}$, $h_S \in \{0.1, 0.5\}$, $W = \{0.1, 0.3, 0.6, 0.9\}$, $ATS_0 = 370.4$

	$n = 3$								
	FSI	VSI							
	$h_L = 1$	$h_S = 0.5$				$h_S = 0.1$			
		W				W			
τ		0.9	0.6	0.3	0.1	0.9	0.6	0.3	0.1
0.60	17.8	12.7	12.6	12.2	11.9	7.9	7.5	7.7	6.8
0.70	28.5	21.0	20.3	20.0	19.9	14.4	13.4	12.3	11.9
0.80	54.3	41.9	40.3	39.4	39.1	31.7	28.9	27.2	26.7
0.90	155.8	136.1	132.2	129.7	128.9	120.3	113.3	108.8	107.4
0.95	325.7	313.1	310.1	308.0	307.4	303.2	297.8	294.1	293.0
1.05	153.6	146.1	144.8	144.0	143.8	140.1	137.9	136.5	136.1
1.10	64.9	55.4	54.0	53.0	52.8	47.8	45.2	43.6	43.1
1.20	21.6	14.7	14.0	13.6	13.4	9.2	7.9	7.1	6.9
1.30	11.6	6.8	6.5	6.4	6.3	3.0	2.5	2.2	2.1
1.40	7.8	4.3	4.1	4.0	4.0	1.5	1.2	1.1	1.0
1.50	5.9	3.1	3.0	3.0	3.0	0.9	0.7	0.7	0.7
1.60	4.8	2.5	2.4	2.4	2.4	0.6	0.5	0.5	0.5
1.70	4.0	2.1	2.0	2.0	2.0	0.5	0.4	0.4	0.4
1.80	3.5	1.8	1.8	1.8	1.8	0.4	0.4	0.4	0.4
1.90	3.1	1.6	1.6	1.6	1.6	0.3	0.3	0.3	0.3
2.00	2.9	1.4	1.4	1.4	1.4	0.3	0.3	0.3	0.3
	$n = 5$								
	FSI	VSI							
	$h_L = 1$	$h_S = 0.5$				$h_S = 0.1$			
		W				W			
τ		0.9	0.6	0.3	0.1	0.9	0.6	0.3	0.1
0.60	9.0	6.8	5.9	5.7	5.7	4.5	3.2	2.4	2.4
0.70	14.6	11.0	10.2	10.2	10.2	7.7	5.9	5.6	5.5
0.80	28.2	21.3	20.8	20.3	20.2	15.6	14.5	13.8	13.6
0.90	81.0	67.6	65.3	63.9	63.5	56.9	52.8	50.2	49.4
0.95	202.9	189.9	187.0	185.1	184.5	179.4	174.3	170.8	169.8
1.05	121.4	111.1	109.1	107.9	107.5	102.9	99.4	97.2	96.5
1.10	44.8	34.8	33.3	32.4	32.1	26.9	24.1	22.4	21.9
1.20	15.3	9.3	8.8	8.5	8.4	4.6	3.6	3.1	3.0
1.30	8.8	4.8	4.6	4.5	4.5	1.7	1.3	1.1	1.1
1.40	6.2	3.3	3.2	3.1	3.1	1.0	0.8	0.7	0.7
1.50	4.8	2.5	2.4	2.4	2.4	0.7	0.5	0.5	0.5
1.60	4.0	2.0	2.0	2.0	2.0	0.5	0.4	0.4	0.4
1.70	3.5	1.8	1.7	1.7	1.7	0.4	0.4	0.3	0.3
1.80	2.9	1.6	1.5	1.5	1.5	0.3	0.3	0.3	0.3
1.90	2.5	1.4	1.4	1.4	1.4	0.3	0.3	0.3	0.3
2.00	2.3	1.3	1.3	1.3	1.3	0.3	0.3	0.3	0.3

Table 17.11 Optimal out-of-control ATS^* of the VSI EWMA-S^2 for $\tau \in \{0.6, 0.7, 0.8, 0.9, 0.95, 1.05, 1.1, 1.2, \ldots, 2\}$, $n \in \{7, 9\}$, $h_S \in \{0.1, 0.5\}$, $W = \{0.1, 0.3, 0.6, 0.9\}$, $ATS_0 = 370.4$

	$n=7$								
	FSI	VSI							
	$h_L = 1$	$h_S = 0.5$				$h_S = 0.1$			
		W				W			
τ		0.9	0.6	0.3	0.1	0.9	0.6	0.3	0.1
0.60	6.2	4.6	4.6	3.5	3.5	3.0	3.0	1.2	1.1
0.70	10.0	7.5	7.0	6.5	6.5	5.2	4.6	3.1	3.0
0.80	19.5	15.1	14.1	14.0	14.0	11.1	9.2	8.8	8.7
0.90	56.8	46.5	45.0	44.0	43.7	38.4	35.5	33.7	33.2
0.95	150.6	137.7	135.1	133.2	132.7	127.5	122.7	119.4	118.4
1.05	99.3	95.2	92.9	91.3	90.9	79.3	75.4	72.8	72.1
1.10	34.9	27.3	25.7	24.8	24.5	18.3	15.7	14.2	13.7
1.20	12.4	7.8	7.3	7.0	7.0	3.4	2.5	2.1	2.0
1.30	7.4	4.3	4.0	4.0	3.9	1.4	1.0	0.9	0.9
1.40	5.3	3.0	2.9	2.8	2.8	0.8	0.6	0.6	0.6
1.50	4.2	2.3	2.2	2.2	2.2	0.6	0.5	0.4	0.4
1.60	3.2	1.9	1.9	1.9	1.9	0.5	0.4	0.4	0.4
1.70	2.6	1.6	1.6	1.6	1.6	0.4	0.3	0.3	0.3
1.80	2.2	1.5	1.5	1.4	1.4	0.3	0.3	0.3	0.3
1.90	2.0	1.3	1.3	1.3	1.3	0.3	0.3	0.3	0.3
2.00	1.8	1.2	1.2	1.2	1.2	0.3	0.2	0.2	0.2
	$n=9$								
	FSI	VSI							
	$h_L = 1$	$h_S = 0.5$				$h_S = 0.1$			
		W				W			
τ		0.9	0.6	0.3	0.1	0.9	0.6	0.3	0.1
0.60	4.7	3.5	3.7	2.5	2.5	2.4	2.8	0.7	0.7
0.70	7.7	5.8	5.9	4.7	4.7	3.9	4.1	2.0	1.9
0.80	15.1	11.5	10.8	10.5	10.5	8.4	7.4	6.1	6.1
0.90	44.7	36.3	34.9	34.1	33.9	29.6	27.0	25.7	25.3
0.95	120.9	108.6	106.1	104.4	103.9	98.7	94.3	91.3	90.3
1.05	84.0	72.7	70.5	69.0	68.5	63.6	59.6	56.9	56.1
1.10	29.0	20.6	19.3	18.5	18.3	13.8	11.5	10.1	9.7
1.20	10.7	6.3	5.9	5.7	5.6	2.8	2.0	1.6	1.5
1.30	6.6	3.6	3.4	3.3	3.3	1.2	0.9	0.8	0.7
1.40	4.7	2.6	2.5	2.4	2.4	0.8	0.6	0.5	0.5
1.50	3.4	2.0	2.0	1.9	1.9	0.5	0.4	0.4	0.4
1.60	2.7	1.7	1.6	1.6	1.6	0.4	0.3	0.3	0.3
1.70	2.2	1.5	1.4	1.4	1.4	0.3	0.3	0.3	0.3
1.80	1.9	1.3	1.3	1.3	1.3	0.3	0.3	0.3	0.3
1.90	1.6	1.2	1.2	1.2	1.2	0.3	0.2	0.2	0.2
2.00	1.5	1.1	1.1	1.1	1.1	0.2	0.2	0.2	0.2

17.4.3 Average Time to Signal for a VSI Control Chart

If the *ARL* is a useful tool for comparing the performance of various control charts, this indicator cannot be used in the case of VSI-type control charts since the interval between two consecutive samples is not constant. As a consequence, it is common to use the *average time to signal* (*ATS*): when the process is in-control and remains in this state, it is desirable to have

Table 17.12 Optimal h_L^* values of the VSI EWMA-S^2 for $n \in \{3, 5, 7, 9\}$, $\tau \in \{0.6, 0.7, 0.8, 0.9, 0.95, 1.05, 1.1, 1.2, \ldots, 2\}$, $h_S \in \{0.1, 0.5\}$, $W = \{0.1, 0.3, 0.6, 0.9\}$, $ATS_0 = 370.4$

	$n = 3$								$n = 5$							
	$h_S = 0.5$				$h_S = 0.1$				$h_S = 0.5$				$h_S = 0.1$			
	W				W				W				W			
τ	0.9	0.6	0.3	0.15	0.9	0.6	0.3	0.15	0.9	0.6	0.3	0.15	0.9	0.6	0.3	0.15
0.60	1.30	1.59	2.67	4.46	1.52	2.16	3.94	7.23	1.28	1.64	2.61	4.39	1.51	2.15	3.92	7.13
0.70	1.28	1.60	2.69	4.56	1.54	2.06	4.00	7.23	1.29	1.57	2.62	4.40	1.51	2.15	3.91	7.10
0.80	1.27	1.56	2.46	4.65	1.48	2.01	3.63	7.56	1.27	1.60	2.68	4.51	1.49	2.05	4.00	7.27
0.90	1.27	1.57	2.48	4.70	1.49	2.03	3.67	7.66	1.27	1.57	2.49	4.71	1.49	2.03	3.68	7.67
0.95	1.27	1.57	2.48	4.70	1.49	2.03	3.67	7.66	1.27	1.57	2.49	4.71	1.49	2.03	3.68	7.67
1.05	1.27	1.57	2.48	4.70	1.49	2.03	3.67	7.66	1.27	1.57	2.49	4.71	1.49	2.03	3.68	7.67
1.10	1.27	1.57	2.48	4.70	1.49	2.03	3.67	7.66	1.27	1.57	2.49	4.71	1.49	2.03	3.68	7.67
1.20	1.27	1.57	2.48	4.70	1.49	2.03	3.67	7.66	1.27	1.57	2.49	4.71	1.49	2.03	3.68	7.67
1.30	1.27	1.57	2.48	4.70	1.49	2.03	3.67	7.66	1.27	1.57	2.49	4.71	1.49	2.03	3.68	7.67
1.40	1.27	1.57	2.48	4.70	1.49	2.03	3.67	7.66	1.27	1.57	2.49	4.71	1.49	2.03	3.68	7.67
1.50	1.27	1.57	2.48	4.70	1.49	2.03	3.67	7.66	1.27	1.57	2.49	4.71	1.49	2.03	3.68	7.67
1.60	1.27	1.57	2.48	4.70	1.49	2.03	3.67	7.66	1.27	1.57	2.49	4.71	1.49	2.03	3.68	7.67
1.70	1.27	1.57	2.48	4.70	1.49	2.03	3.67	7.66	1.27	1.57	2.49	4.71	1.49	2.03	3.68	7.67
1.80	1.27	1.57	2.48	4.70	1.49	2.03	3.67	7.66	1.27	1.57	2.49	4.71	1.49	2.03	3.68	7.67
1.90	1.27	1.57	2.48	4.70	1.49	2.03	3.67	7.66	1.27	1.57	2.49	4.71	1.49	2.03	3.68	7.67
2.00	1.27	1.57	2.48	4.70	1.49	2.03	3.67	7.66	1.27	1.57	2.49	4.71	1.49	2.03	3.68	7.67

	$n = 7$								$n = 9$							
	$h_S = 0.5$				$h_S = 0.1$				$h_S = 0.5$				$h_S = 0.1$			
	W				W				W				W			
τ	0.9	0.6	0.3	0.15	0.9	0.6	0.3	0.15	0.9	0.6	0.3	0.15	0.9	0.6	0.3	0.15
0.60	1.28	1.57	2.60	4.35	1.51	2.02	3.92	7.11	1.27	1.62	2.58	4.32	1.50	2.03	3.87	7.03
0.70	1.28	1.57	2.60	4.35	1.50	2.02	3.87	7.06	1.27	1.62	2.58	4.32	1.49	2.03	3.85	6.98
0.80	1.26	1.58	2.62	4.41	1.51	2.02	3.88	7.05	1.28	1.57	2.59	4.35	1.50	2.03	3.86	7.00
0.90	1.27	1.57	2.48	4.69	1.49	2.03	3.67	7.65	1.27	1.55	2.44	4.61	1.48	2.09	4.06	7.50
0.95	1.27	1.57	2.48	4.69	1.49	2.03	3.67	7.65	1.27	1.57	2.48	4.68	1.48	2.02	3.66	7.63
1.05	1.27	1.57	2.48	4.69	1.49	2.03	3.67	7.65	1.27	1.57	2.48	4.68	1.48	2.02	3.66	7.63
1.10	1.27	1.57	2.48	4.69	1.49	2.03	3.67	7.65	1.27	1.57	2.48	4.68	1.48	2.02	3.66	7.63
1.20	1.27	1.57	2.48	4.69	1.49	2.03	3.67	7.65	1.27	1.57	2.48	4.68	1.48	2.02	3.66	7.63
1.30	1.27	1.57	2.48	4.69	1.49	2.03	3.67	7.65	1.27	1.57	2.48	4.68	1.48	2.02	3.66	7.63
1.40	1.27	1.57	2.48	4.69	1.49	2.03	3.67	7.65	1.27	1.57	2.48	4.68	1.48	2.02	3.66	7.63
1.50	1.27	1.57	2.48	4.69	1.49	2.03	3.67	7.65	1.27	1.57	2.48	4.68	1.48	2.02	3.66	7.63
1.60	1.27	1.57	2.48	4.69	1.49	2.03	3.67	7.65	1.27	1.57	2.48	4.68	1.48	2.02	3.66	7.63
1.70	1.27	1.57	2.48	4.69	1.49	2.03	3.67	7.65	1.27	1.57	2.48	4.68	1.48	2.02	3.66	7.63
1.80	1.27	1.57	2.48	4.69	1.49	2.03	3.67	7.65	1.27	1.57	2.48	4.68	1.48	2.02	3.66	7.63
1.90	1.27	1.57	2.48	4.69	1.49	2.03	3.67	7.65	1.27	1.57	2.48	4.68	1.48	2.02	3.66	7.63
2.00	1.27	1.57	2.48	4.69	1.49	2.03	3.67	7.65	1.27	1.57	2.48	4.68	1.48	2.02	3.66	7.63

Table 17.13 Optimal couples (λ^*, K^*) of the VSI EWMA-S^2 for $n \in \{3, 5\}$, $\tau \in \{0.6, 0.7, 0.8, 0.9, 0.95, 1.05, 1.1, 1.2, \ldots, 2\}$, $h_S \in \{0.1, 0.5\}$, $W = \{0.1, 0.3, 0.6, 0.9\}$, $ATS_0 = 370.4$

	$n=3$															
	$h_S = 0.5$								**$h_S = 0.1$**							
	W								**W**							
	0.9		**0.6**		**0.3**		**0.15**		**0.9**		**0.6**		**0.3**		**0.15**	
τ	λ^*	K^*	λ^*	K^*	λ^*	K^*	λ^*	K^*	λ^*	K^*	λ^*	K^*	λ^*	K^*	λ^*	K^*
0.60	0.13	2.742	0.12	2.726	0.11	2.709	0.13	2.742	0.16	2.779	0.19	2.808	0.16	2.779	0.13	2.742
0.70	0.09	2.669	0.09	2.669	0.09	2.669	0.08	2.643	0.12	2.726	0.11	2.709	0.11	2.709	0.13	2.742
0.80	0.05	2.548	0.06	2.583	0.06	2.583	0.06	2.583	0.06	2.583	0.06	2.583	0.06	2.583	0.06	2.583
0.90	0.05	2.548	0.05	2.548	0.05	2.548	0.05	2.548	0.05	2.548	0.05	2.548	0.05	2.548	0.05	2.548
0.95	0.05	2.548	0.05	2.548	0.05	2.548	0.05	2.548	0.05	2.548	0.05	2.548	0.05	2.548	0.05	2.548
1.05	0.05	2.548	0.05	2.548	0.05	2.548	0.05	2.548	0.05	2.548	0.05	2.548	0.05	2.548	0.05	2.548
1.10	0.05	2.548	0.05	2.548	0.05	2.548	0.05	2.548	0.05	2.548	0.05	2.548	0.05	2.548	0.05	2.548
1.20	0.05	2.548	0.05	2.548	0.05	2.548	0.05	2.548	0.05	2.548	0.05	2.548	0.05	2.548	0.05	2.548
1.30	0.05	2.548	0.05	2.548	0.05	2.548	0.05	2.548	0.05	2.548	0.05	2.548	0.05	2.548	0.05	2.548
1.40	0.05	2.548	0.05	2.548	0.05	2.548	0.05	2.548	0.05	2.548	0.05	2.548	0.05	2.548	0.05	2.548
1.50	0.05	2.548	0.05	2.548	0.05	2.548	0.05	2.548	0.05	2.548	0.05	2.548	0.05	2.548	0.05	2.548
1.60	0.05	2.548	0.05	2.548	0.05	2.548	0.05	2.548	0.05	2.548	0.05	2.548	0.05	2.548	0.05	2.548
1.70	0.05	2.548	0.05	2.548	0.05	2.548	0.05	2.548	0.05	2.548	0.05	2.548	0.05	2.548	0.05	2.548
1.80	0.05	2.548	0.05	2.548	0.05	2.548	0.05	2.548	0.05	2.548	0.05	2.548	0.05	2.548	0.05	2.548
1.90	0.05	2.548	0.05	2.548	0.05	2.548	0.05	2.548	0.05	2.548	0.05	2.548	0.05	2.548	0.05	2.548
2.00	0.05	2.548	0.05	2.548	0.05	2.548	0.05	2.548	0.05	2.548	0.05	2.548	0.05	2.548	0.05	2.548
	$n=5$															
	$h_S = 0.5$								**$h_S = 0.1$**							
	W								**W**							
	0.9		**0.6**		**0.3**		**0.15**		**0.9**		**0.6**		**0.3**		**0.15**	
τ	λ^*	K^*	λ^*	K^*	λ^*	K^*	λ^*	K^*	λ^*	K^*	λ^*	K^*	λ^*	K^*	λ^*	K^*
0.60	0.21	2.808	0.22	2.812	0.24	2.820	0.24	2.820	0.31	2.833	0.23	2.816	0.31	2.833	0.31	2.833
0.70	0.15	2.763	0.15	2.763	0.17	2.782	0.17	2.782	0.19	2.797	0.21	2.808	0.24	2.820	0.24	2.820
0.80	0.09	2.663	0.09	2.663	0.09	2.663	0.09	2.663	0.10	2.687	0.11	2.707	0.10	2.687	0.10	2.687
0.90	0.05	2.515	0.05	2.515	0.05	2.515	0.05	2.515	0.05	2.515	0.05	2.515	0.05	2.515	0.05	2.515
0.95	0.05	2.515	0.05	2.515	0.05	2.515	0.05	2.515	0.05	2.515	0.05	2.515	0.05	2.515	0.05	2.515
1.05	0.05	2.515	0.05	2.515	0.05	2.515	0.05	2.515	0.05	2.515	0.05	2.515	0.05	2.515	0.05	2.515
1.10	0.05	2.515	0.05	2.515	0.05	2.515	0.05	2.515	0.05	2.515	0.05	2.515	0.05	2.515	0.05	2.515
1.20	0.05	2.515	0.05	2.515	0.05	2.515	0.05	2.515	0.05	2.515	0.05	2.515	0.05	2.515	0.05	2.515
1.30	0.05	2.515	0.05	2.515	0.05	2.515	0.05	2.515	0.05	2.515	0.05	2.515	0.05	2.515	0.05	2.515
1.40	0.05	2.515	0.05	2.515	0.05	2.515	0.05	2.515	0.05	2.515	0.05	2.515	0.05	2.515	0.05	2.515
1.50	0.05	2.515	0.05	2.515	0.05	2.515	0.05	2.515	0.05	2.515	0.05	2.515	0.05	2.515	0.05	2.515
1.60	0.05	2.515	0.05	2.515	0.05	2.515	0.05	2.515	0.05	2.515	0.05	2.515	0.05	2.515	0.05	2.515
1.70	0.05	2.515	0.05	2.515	0.05	2.515	0.05	2.515	0.05	2.515	0.05	2.515	0.05	2.515	0.05	2.515
1.80	0.05	2.515	0.05	2.515	0.05	2.515	0.05	2.515	0.05	2.515	0.05	2.515	0.05	2.515	0.05	2.515
1.90	0.05	2.515	0.05	2.515	0.05	2.515	0.05	2.515	0.05	2.515	0.05	2.515	0.05	2.515	0.05	2.515
2.00	0.05	2.515	0.05	2.515	0.05	2.515	0.05	2.515	0.05	2.515	0.05	2.515	0.05	2.515	0.05	2.515

a large *ATS* since it represents the expected value of the elapsed time between two consecutive false alarms. Otherwise, if the characteristic of the process has shifted, it is desirable to have an *ATS* that is as small as possible. Since it represents the expected value of the elapsed time between the occurence of a special cause,

Table 17.14 Optimal couples (λ^*, K^*) of the VSI EWMA-S^2 for $n \in \{7, 9\}$, $\tau \in \{0.6, 0.7, 0.8, 0.9, 0.95, 1.05, 1.1, 1.2, \dots, 2\}$, $h_S \in \{0.1, 0.5\}$, $W = \{0.1, 0.3, 0.6, 0.9\}$, $ATS_0 = 370.4$

	$n = 7$															
	$h_S = 0.5$								$h_S = 0.1$							
	W								W							
	0.9		0.6		0.3		0.15		0.9		0.6		0.3		0.15	
τ	λ^*	K^*	λ^*	K^*	λ^*	K^*	λ^*	K^*	λ^*	K^*	λ^*	K^*	λ^*	K^*	λ^*	K^*
0.60	0.33	2.849	0.15	2.771	0.28	2.843	0.28	2.843	0.41	2.848	0.15	2.771	0.41	2.848	0.41	2.848
0.70	0.20	2.813	0.15	2.771	0.20	2.813	0.24	2.833	0.28	2.843	0.15	2.771	0.28	2.843	0.33	2.849
0.80	0.11	2.710	0.11	2.710	0.13	2.745	0.13	2.745	0.14	2.759	0.14	2.759	0.18	2.800	0.18	2.800
0.90	0.05	2.506	0.05	2.506	0.05	2.506	0.05	2.506	0.05	2.506	0.05	2.506	0.05	2.506	0.05	2.506
0.95	0.05	2.506	0.05	2.506	0.05	2.506	0.05	2.506	0.05	2.506	0.05	2.506	0.05	2.506	0.05	2.506
1.05	0.05	2.506	0.05	2.506	0.05	2.506	0.05	2.506	0.05	2.506	0.05	2.506	0.05	2.506	0.05	2.506
1.10	0.05	2.506	0.05	2.506	0.05	2.506	0.05	2.506	0.05	2.506	0.05	2.506	0.05	2.506	0.05	2.506
1.20	0.05	2.506	0.05	2.506	0.05	2.506	0.05	2.506	0.05	2.506	0.05	2.506	0.05	2.506	0.05	2.506
1.30	0.05	2.506	0.05	2.506	0.05	2.506	0.05	2.506	0.05	2.506	0.05	2.506	0.05	2.506	0.05	2.506
1.40	0.05	2.506	0.05	2.506	0.05	2.506	0.05	2.506	0.05	2.506	0.05	2.506	0.05	2.506	0.05	2.506
1.50	0.05	2.506	0.05	2.506	0.05	2.506	0.05	2.506	0.05	2.506	0.05	2.506	0.05	2.506	0.05	2.506
1.60	0.05	2.506	0.05	2.506	0.05	2.506	0.05	2.506	0.05	2.506	0.05	2.506	0.05	2.506	0.05	2.506
1.70	0.05	2.506	0.05	2.506	0.05	2.506	0.05	2.506	0.05	2.506	0.05	2.506	0.05	2.506	0.05	2.506
1.80	0.05	2.506	0.05	2.506	0.05	2.506	0.05	2.506	0.05	2.506	0.05	2.506	0.05	2.506	0.05	2.506
1.90	0.05	2.506	0.05	2.506	0.05	2.506	0.05	2.506	0.05	2.506	0.05	2.506	0.05	2.506	0.05	2.506
2.00	0.05	2.506	0.05	2.506	0.05	2.506	0.05	2.506	0.05	2.506	0.05	2.506	0.05	2.506	0.05	2.506
	$n = 9$															
	$h_S = 0.5$								$h_S = 0.1$							
	W								W							
	0.9		0.6		0.3		0.15		0.9		0.6		0.3		0.15	
τ	λ^*	K^*	λ^*	K^*	λ^*	K^*	λ^*	K^*	λ^*	K^*	λ^*	K^*	λ^*	K^*	λ^*	K^*
0.60	0.33	2.865	0.34	2.866	0.33	2.865	0.33	2.865	0.46	2.864	0.12	2.733	0.41	2.868	0.54	2.854
0.70	0.27	2.854	0.27	2.854	0.27	2.854	0.27	2.854	0.33	2.865	0.12	2.733	0.38	2.868	0.42	2.867
0.80	0.15	2.777	0.12	2.733	0.17	2.798	0.17	2.798	0.17	2.798	0.12	2.733	0.23	2.839	0.23	2.839
0.90	0.05	2.502	0.06	2.555	0.06	2.555	0.06	2.555	0.05	2.502	0.07	2.599	0.07	2.599	0.06	2.555
0.95	0.05	2.502	0.05	2.502	0.05	2.502	0.05	2.502	0.05	2.502	0.05	2.502	0.05	2.502	0.05	2.502
1.05	0.05	2.502	0.05	2.502	0.05	2.502	0.05	2.502	0.05	2.502	0.05	2.502	0.05	2.502	0.05	2.502
1.10	0.05	2.502	0.05	2.502	0.05	2.502	0.05	2.502	0.05	2.502	0.05	2.502	0.05	2.502	0.05	2.502
1.20	0.05	2.502	0.05	2.502	0.05	2.502	0.05	2.502	0.05	2.502	0.05	2.502	0.05	2.502	0.05	2.502
1.30	0.05	2.502	0.05	2.502	0.05	2.502	0.05	2.502	0.05	2.502	0.05	2.502	0.05	2.502	0.05	2.502
1.40	0.05	2.502	0.05	2.502	0.05	2.502	0.05	2.502	0.05	2.502	0.05	2.502	0.05	2.502	0.05	2.502
1.50	0.05	2.502	0.05	2.502	0.05	2.502	0.05	2.502	0.05	2.502	0.05	2.502	0.05	2.502	0.05	2.502
1.60	0.05	2.502	0.05	2.502	0.05	2.502	0.05	2.502	0.05	2.502	0.05	2.502	0.05	2.502	0.05	2.502
1.70	0.05	2.502	0.05	2.502	0.05	2.502	0.05	2.502	0.05	2.502	0.05	2.502	0.05	2.502	0.05	2.502
1.80	0.05	2.502	0.05	2.502	0.05	2.502	0.05	2.502	0.05	2.502	0.05	2.502	0.05	2.502	0.05	2.502
1.90	0.05	2.502	0.05	2.502	0.05	2.502	0.05	2.502	0.05	2.502	0.05	2.502	0.05	2.502	0.05	2.502
2.00	0.05	2.502	0.05	2.502	0.05	2.502	0.05	2.502	0.05	2.502	0.05	2.502	0.05	2.502	0.05	2.502

i. e. the transition of the process to an out-of-control state, and the signal from the control chart. For an FSI model, the *ATS* is a multiple of the *ARL* since the time h_F between samples is fixed. Thus, in this case we have

$$ATS^{FSI} = h_F \times ARL^{FSI} .$$

For a VSI model, the *ATS* depends on both the number of samples to signal (the *ARL*) and the sampling frequency, which is variable,

$$ATS^{VSI} = E(h) \times ARL^{VSI} ,$$

where $E(h)$ represents the expected value of the sampling interval. For given λ and K, the value of $E(h)$ depends on W, h_S and h_L. For fixed values of h_S and $E(h)$, with $h_S < E(h)$, there is (see *Reynolds* [17.35]) a one-to-one correspondence between W and h_L such that, if the first one decreases, the second one has to increase, and conversely. If we have to compare the out-of-control *ATS* performance of two FSI-type control charts, we only need to define them with the same in-control $ARL_Y = ARL_0$. For VSI-type control charts, this is a little more complex because, if one control chart samples the process more frequently than another, it will necessarily detect a shift in the process sooner than the other one. Consequently, if we have to compare the out-of-control *ATS* performance of two VSI-type control charts, we need to define them with the same in-control $ARL_Y = ARL_0$ *and* the same in-control average sampling interval $E_0(h)$. Because, for *FSI*-type control charts, we have $h_S = h_L = h_F = 1$ time units, the in-control average sampling interval is chosen to be $E_0(h) = 1$. This ensures that we have the same $ATS_Y = ATS_0$ for both FSI- and VSI-type control charts.

17.4.4 Performance of the VSI EWMA-S^2 Control Chart

The performance of the VSI EWMA-S^2 control chart has been investigated by *Castagliola* et al. [17.36]. The *ATS* of the VSI EWMA-S^2 control chart can be computed using the second approach presented in Sect. 17.2.3, where the element g_j of the $(p, 1)$ vector $\boldsymbol{g}$ is defined by

$$g_j = \begin{cases} h_L & \text{if } LWL < H_j < UWL \\ h_S & \text{otherwise} \end{cases} .$$

The optimization scheme of the VSI EWMA-S^2 control chart consists of finding the optimal combination (λ^*, K^*, h_L^*) that give the same in-control $ATS_Y = ATS_0$ (i. e. the *ATS* when the process is functioning at the nominal variability $\sigma = \sigma_0$ or equivalently $\tau = 1$) and then, for predefined values of τ, W and h_S, find the unique combination (λ^*, K^*, h_L^*) which yields the smallest possible out-of-control $ATS_Y = ATS^*$, subject to the constraint $E_0(h) = 1$. The minimal *ATS* values achieved using the optimal VSI model are summarized in Table 17.10 and Table 17.11 for shift $\tau \in \{0.6, 0.7, 0.8, 0.9, 0.95, 1.05, 1.1, 1.2, \dots, 2\}$ and $n \in \{3, 5, 7, 9\}$. The values used for h_S are 0.5 and 0.1 time units. For comparison purposes, Tables 17.10 and 17.11 also show the minimal *ATS* of the FSI EWMA-S^2 (column $h_L = 1$). As expected, the results clearly indicate that the VSI model outperforms the FSI scheme for all considered shifts of variability since the VSI model gives a signal earlier than the FSI model. For example, for $n = 5$, $h_S = 0.5$ and $W = 0.6$ we have $ATS^* = 65.3$ when $\tau = 0.9$, while for the FSI model we have $ATS^* = 81.0$. When $\tau = 1.2$, we have $ATS^* = 8.8$ for the VSI EWMA-S^2 control chart, while for the FSI model we have $ATS^* = 15.3$. We can also notice that the performance in term of *ATS* is improved when a smaller short sampling interval h_S is considered and, for a selected value of h_S, the *ATS* is improved as the value of W decreases. Table 17.12 shows the optimal long sampling interval h_L^* for several combinations of n, W, h_S and τ. For a defined value of h_S, when W decreases it is no surprise to remark that the length of the long sampling interval h_L^* increases. Finally, Tables 17.13 and 17.14 summarize the optimal couples (λ^*, K^*).

Example 17.6: The goal of this example is to illustrate the use of the VSI EWMA-S^2 control chart using a simulated process. The sample size is assumed to be $n = 5$. We assume that during the first 20 units of time the data are generated according to a normal $(20, 0.1)$ distribution (corresponding to an in-control process) while, after the first 20 units of time, the data are generated according to a normal $(20, 0.13)$ distribution (the nominal process standard deviation σ_0 has increased by a factor of 1.3). If $n = 5$ and $\sigma_0 = 0.1$, then we deduce from Table 17.3: $b_{S^2} = 2.3647$, $c_{S^2} = 0.5979 \times 0.1^2 = 0.005\,979$ and $a_{S^2} = -0.8969 - 2 \times 2.3647 \times \ln(0.1) = 9.9929$. The FSI EWMA chart has been designed by considering $\lambda = 0.05$, $K = 2.515$ and $h_F = 1$; the VSI EWMA was implemented by considering the same couple (λ, K) and $h_S = 0.5$, $h_L = 1.27$, $W = 0.9$. This choice ensures that both the FSI and VSI EWMA-S^2 control charts are designed to have the

Table 17.15 Subgroup number, sampling interval (h_S or h_L), total elapsed time from the start of the simulation and statistics S_k^2, T_k and Y_k

Subgroup	Sampling interval	Total time	S_k^2	T_k	Y_k
1	0.50	0.50	0.003 38	−1.052	0.148
2	0.50	1.00	0.003 15	−1.112	0.085
3	1.27	2.27	0.018 55	1.225	0.142
4	1.27	3.54	0.002 54	−1.275	0.071
5	1.27	4.81	0.004 52	−0.782	0.028
6	1.27	6.08	0.003 76	−0.959	−0.021
7	1.27	7.35	0.009 34	0.112	−0.014
8	1.27	8.62	0.008 53	−0.017	−0.014
9	1.27	9.89	0.017 23	1.094	0.041
10	1.27	11.16	0.008 61	−0.003	0.039
11	1.27	12.43	0.027 72	1.976	0.136
12	1.27	13.70	0.014 22	0.765	0.167
13	0.50	14.20	0.016 96	1.067	0.212
14	0.50	14.70	0.010 37	0.266	0.215
15	0.50	15.20	0.009 56	0.146	0.211
16	0.50	15.70	0.005 31	−0.610	0.170
17	0.50	16.20	0.008 97	0.053	0.164
18	0.50	16.70	0.008 21	−0.070	0.153
19	0.50	17.20	0.009 76	0.176	0.154
20	0.50	17.70	0.016 04	0.970	0.195
21	0.50	18.20	0.005 95	−0.479	0.161
22	0.50	18.70	0.010 25	0.249	0.165
23	0.50	19.20	0.007 75	−0.148	0.150
24	0.50	19.70	0.011 63	0.441	0.164
25	0.50	20.20	0.012 12	0.507	0.181
26	0.50	20.70	0.030 40	2.157	0.280
27	0.50	21.20	0.019 89	1.351	0.334
28	0.50	21.70	0.016 07	0.973	0.366
29	0.50	22.20	0.013 19	0.641	0.379
30	0.50	22.70	0.001 53	−1.573	0.282
31	0.50	23.20	0.009 95	0.203	0.278
32	0.50	23.70	0.020 19	1.378	0.333
33	0.50	24.20	0.008 90	0.043	0.318
34	0.50	24.70	0.025 98	1.850	0.395
35	0.50	25.20	0.019 70	1.333	0.442

same in control $ARL_0 = 370.4$ and are designed to optimally detect a $\tau = 1.5$ shift for the process variability. The control and warning limits are $LCL = 0.0075 - 2.515\sqrt{0.05/1.95} \times 0.967 = -0.382$, $UCL = 0.0075 + 2.515\sqrt{0.05/1.95} \times 0.967 = 0.397$, $LWL = 0.0075 - 0.9\sqrt{0.05/1.95} \times 0.967 = -0.132$ and $UWL = 0.0075 + 0.9\sqrt{0.05/1.95} \times 0.967 = 0.147$. In Table 17.15 we summarize the results of this simulation, i. e. the subgroup number, the sampling interval (h_S or h_L) used for each sample, the total elapsed time from the start of the process simulation and the statistics S_k^2, T_k and Y_k. In Fig. 17.18 (top), we plot the VSI EWMA-S^2 control chart (i. e. the Y_ks) corresponding to our data. As we can see, the VSI EWMA-S^2 control chart clearly detects an out-of-control signal after 25.2 units of time (35-th subgroup), pointing out that an increase of the variance occurred. In Fig. 17.18 (bottom), we plotted the FSI EWMA-S^2 control chart using the same data but

Table 17.16 Optimal out-of-control ATS^* of the VSI EWMA-R for $\tau \in \{0.6, 0.7, 0.8, 0.9, 0.95, 1.05, 1.1, 1.2, \ldots, 2\}$, $n \in \{3, 5\}$, $h_S \in \{0.1, 0.5\}$, $W = \{0.1, 0.3, 0.6, 0.9\}$, $ATS_0 = 370.4$

	$n = 3$								
	FSI	VSI							
	$h_L = 1$	$h_S = 0.5$				$h_S = 0.1$			
		W				W			
τ		0.9	0.6	0.3	0.1	0.9	0.6	0.3	0.1
0.60	15.0	11.1	11.3	10.2	10.1	7.7	7.7	5.5	5.2
0.70	24.5	18.9	18.7	17.8	17.8	13.9	13.7	11.3	11.2
0.80	46.6	38.0	36.4	35.8	35.6	31.0	27.9	26.9	26.7
0.90	133.9	121.6	118.6	116.9	116.4	112.0	106.6	103.5	102.6
0.95	274.9	267.7	265.9	264.8	264.5	262.4	259.2	257.2	256.6
1.05	198.1	192.0	190.1	189.0	188.7	186.9	183.5	181.5	180.9
1.10	94.7	86.4	83.9	82.5	82.1	79.4	74.8	72.3	71.6
1.20	35.8	29.2	27.2	26.2	25.9	23.7	20.0	18.3	17.8
1.30	20.4	15.7	14.1	13.4	13.3	11.8	8.8	7.7	7.4
1.40	14.2	10.6	9.2	8.8	8.6	7.6	5.1	4.3	4.1
1.50	10.7	8.1	6.8	6.5	6.4	5.7	3.5	2.8	2.7
1.60	8.2	6.6	5.4	5.2	5.1	4.6	2.6	2.1	1.9
1.70	6.5	5.6	4.5	4.3	4.2	3.9	2.0	1.6	1.5
1.80	5.4	4.7	3.9	3.7	3.7	3.5	1.6	1.3	1.2
1.90	4.6	4.1	3.4	3.2	3.1	3.1	1.4	1.1	1.0
2.00	4.0	3.6	3.1	2.8	2.7	2.9	1.2	1.0	0.9
	$n = 5$								
	FSI	VSI							
	$h_L = 1$	$h_S = 0.5$				$h_S = 0.1$			
		W				W			
τ		0.9	0.6	0.3	0.1	0.9	0.6	0.3	0.1
0.60	8.2	6.0	6.1	5.6	4.9	4.0	4.2	3.4	1.9
0.70	13.4	10.0	10.1	9.2	8.9	7.0	7.0	5.7	4.7
0.80	25.9	20.2	20.1	19.0	19.1	15.4	15.1	12.8	12.8
0.90	75.0	64.7	63.4	61.5	61.2	56.4	54.1	50.7	50.2
0.95	188.4	179.1	177.4	175.5	175.1	171.7	168.6	165.2	164.5
1.05	149.3	140.9	139.1	137.0	136.6	134.0	130.9	127.2	126.4
1.10	60.5	52	50.5	48.3	47.9	45.1	42.4	38.4	37.7
1.20	22.5	17.3	16.6	14.9	14.7	13.1	11.9	8.8	8.5
1.30	13.3	9.9	9.6	8.1	8.0	7.2	6.6	3.9	3.7
1.40	9.0	6.9	6.9	5.5	5.4	5.0	4.7	2.3	2.1
1.50	6.6	5.2	5.4	4.2	4.1	4.0	3.8	1.6	1.5
1.60	5.1	4.2	4.4	3.3	3.2	3.3	3.3	1.2	1.1
1.70	4.1	3.5	3.7	2.8	2.6	2.9	3.0	0.9	0.9
1.80	3.5	3.0	3.2	2.4	2.1	2.5	2.8	0.8	0.7
1.90	3.0	2.6	2.9	2.1	1.8	2.3	2.6	0.6	0.6
2.00	2.6	2.4	2.7	1.9	1.5	2.2	2.5	0.6	0.5

Table 17.17 Optimal out-of-control ATS^* of the VSI EWMA-R for $\tau \in \{0.6, 0.7, 0.8, 0.9, 0.95, 1.05, 1.1, 1.2, \ldots, 2\}$, $n \in \{7, 9\}$, $h_S \in \{0.1, 0.5\}$, $W = \{0.1, 0.3, 0.6, 0.9\}$, $ATS_0 = 370.4$

	$n = 7$								
	FSI	VSI							
	$h_L = 1$	$h_S = 0.5$				$h_S = 0.1$			
		W				W			
τ		0.9	0.6	0.3	0.1	0.9	0.6	0.3	0.1
0.60	5.9	4.3	4.5	4.4	3.3	2.9	3.2	2.6	1.1
0.70	9.7	7.2	7.3	7.0	6.1	4.9	5.1	4.6	2.8
0.80	19.0	14.5	14.5	13.5	13.3	10.7	10.7	9.1	8.2
0.90	54.9	46.2	45.4	43.9	43.7	39.1	37.7	35.0	34.8
0.95	147.5	137.4	135.6	133.7	133.3	129.3	126.2	122.6	121.9
1.05	122.2	113.0	111.1	108.9	108.4	105.5	102.2	98.2	97.4
1.10	46.5	38.5	37.2	35.2	34.8	32.1	29.8	26.0	25.4
1.20	17.6	13.2	12.7	11.2	11.0	9.8	8.9	6.0	5.7
1.30	10.3	7.8	7.7	6.3	6.2	5.7	5.3	2.7	2.5
1.40	6.9	5.4	5.5	4.3	4.3	4.1	3.9	1.6	1.5
1.50	5.1	4.1	4.3	3.3	3.1	3.2	3.3	1.1	1.0
1.60	4.0	3.3	3.5	2.6	2.3	2.7	2.9	0.8	0.8
1.70	3.3	2.8	3.0	2.2	1.9	2.3	2.7	0.7	0.6
1.80	2.7	2.4	2.7	1.9	1.6	2.1	2.5	0.5	0.5
1.90	2.4	2.2	2.4	1.7	1.4	2.0	2.4	0.5	0.4
2.00	2.1	2.0	2.3	1.5	1.2	1.9	2.3	0.4	0.4
	$n = 9$								
	FSI	VSI							
	$h_L = 1$	$h_S = 0.5$				$h_S = 0.1$			
		W				W			
τ		0.9	0.6	0.3	0.1	0.9	0.6	0.3	0.1
0.60	4.7	3.5	3.7	3.8	2.5	2.4	2.8	2.1	0.8
0.70	7.8	5.8	5.9	6.0	4.6	4.0	4.2	3.9	2.0
0.80	15.4	11.7	11.7	11.1	10.5	8.5	8.5	7.6	6.1
0.90	44.8	37.0	36.5	35.2	35.2	30.7	29.8	27.4	27.3
0.95	123.4	112.8	111.2	109.3	109.0	104.6	101.6	98.2	97.6
1.05	105.4	96.2	94.3	92.1	91.7	88.5	85.2	81.1	80.4
1.10	39.0	31.8	30.7	28.7	28.4	25.8	23.8	20.3	19.7
1.20	15.0	11.3	11.0	9.4	9.3	8.3	7.6	4.9	4.6
1.30	8.7	6.6	6.6	5.3	5.3	4.9	4.7	2.3	2.1
1.40	5.9	4.5	4.7	3.7	3.5	3.4	3.6	1.4	1.2
1.50	4.3	3.4	3.7	2.8	2.5	2.7	3.1	0.9	0.8
1.60	3.4	2.8	3.1	2.3	1.9	2.3	2.7	0.7	0.6
1.70	2.8	2.4	2.7	1.9	1.6	2.1	2.5	0.6	0.5
1.80	2.3	2.1	2.4	1.7	1.3	1.9	2.4	0.5	0.4
1.90	2.0	1.9	2.2	1.5	1.2	1.8	2.3	0.4	0.3
2.00	1.8	1.8	2.1	1.4	1.0	1.7	2.2	0.3	0.3

assuming a fixed sampling rate $h_F = 1$. The difference between the FSI and the VSI EWMA-S^2 control chart appears clearly and, in this example, the difference in terms of detection time is 9.8 units of time.

Table 17.18 Optimal h_L^* values of the VSI EWMA-R for $n \in \{3, 5, 7, 9\}$, $\tau \in \{0.6, 0.7, 0.8, 0.9, 0.95, 1.05, 1.1, 1.2, \ldots, 2\}$, $h_S \in \{0.1, 0.5\}$, $W = \{0.1, 0.3, 0.6, 0.9\}$, $ATS_0 = 370.4$

	$n=3$								$n=5$							
	$h_S=0.5$				$h_S=0.1$				$h_S=0.5$				$h_S=0.1$			
	W				W				W				W			
τ	0.9	0.6	0.3	0.15	0.9	0.6	0.3	0.15	0.9	0.6	0.3	0.15	0.9	0.6	0.3	0.15
0.60	1.28	1.55	2.59	5.05	1.50	2.14	3.86	8.28	1.27	1.61	2.59	4.96	1.54	2.09	3.86	8.09
0.70	1.26	1.60	2.64	5.15	1.51	2.00	3.89	8.34	1.28	1.54	2.59	5.01	1.48	2.11	3.86	8.12
0.80	1.25	1.53	2.39	3.97	1.49	2.07	4.05	8.70	1.26	1.56	2.63	5.14	1.51	1.99	3.89	8.35
0.90	1.25	1.53	2.39	3.97	1.44	1.95	3.51	6.35	1.24	1.52	2.38	3.95	1.44	1.93	3.48	6.30
0.95	1.25	1.53	2.39	3.97	1.44	1.95	3.51	6.35	1.24	1.52	2.38	3.95	1.44	1.93	3.48	6.30
1.05	1.25	1.53	2.39	3.97	1.44	1.95	3.51	6.35	1.24	1.52	2.38	3.95	1.44	1.93	3.48	6.30
1.10	1.25	1.53	2.39	3.97	1.44	1.95	3.51	6.35	1.24	1.52	2.38	3.95	1.44	1.93	3.48	6.30
1.20	1.25	1.53	2.39	3.97	1.44	1.95	3.51	6.35	1.24	1.52	2.38	3.95	1.44	1.93	3.48	6.30
1.30	1.25	1.53	2.39	3.97	1.44	1.95	3.51	6.35	1.24	1.52	2.38	3.95	1.44	1.93	3.48	6.30
1.40	1.25	1.53	2.39	3.97	1.44	1.95	3.51	6.35	1.28	1.52	2.38	3.95	1.44	1.93	3.48	6.30
1.50	1.25	1.53	2.39	3.97	1.44	1.95	3.51	6.35	1.27	1.62	2.38	3.95	1.44	1.93	3.48	6.30
1.60	1.27	1.53	2.39	3.97	1.44	1.95	3.51	6.35	1.30	1.61	2.59	4.94	1.48	1.93	3.48	6.30
1.70	1.28	1.60	2.39	3.97	1.44	1.95	3.51	6.35	1.30	1.61	2.59	4.95	1.48	1.93	3.48	6.30
1.80	1.29	1.60	2.39	3.97	1.44	1.95	3.51	6.35	1.31	1.62	2.59	4.97	1.48	1.93	3.48	6.30
1.90	1.29	1.60	2.59	5.22	1.44	1.95	3.51	6.35	1.31	1.62	2.59	4.97	1.54	1.93	3.48	6.30
2.00	1.29	1.60	2.59	5.36	1.44	1.95	3.51	6.35	1.28	1.63	2.59	4.97	1.55	1.93	3.48	6.30

	$n=7$								$n=9$							
	$h_S=0.5$				$h_S=0.1$				$h_S=0.5$				$h_S=0.1$			
	W				W				W				W			
τ	0.9	0.6	0.3	0.15	0.9	0.6	0.3	0.15	0.9	0.6	0.3	0.15	0.9	0.6	0.3	0.15
0.60	1.30	1.60	2.60	4.90	1.53	3.88	3.88	7.98	1.29	1.59	2.61	4.86	1.52	2.06	3.90	7.93
0.70	1.27	1.61	2.60	4.91	1.54	3.88	3.88	8.02	1.30	1.60	2.61	4.90	1.53	2.07	3.90	7.95
0.80	1.28	1.54	2.60	5.04	1.50	3.88	3.88	8.15	1.28	1.62	2.61	4.98	1.49	2.10	3.90	8.11
0.90	1.24	1.52	2.37	3.94	1.44	3.47	3.47	6.29	1.24	1.52	2.37	3.93	1.48	2.04	4.00	8.59
0.95	1.24	1.52	2.37	3.94	1.44	3.47	3.47	6.29	1.24	1.52	2.37	3.93	1.43	1.93	3.47	6.27
1.05	1.24	1.52	2.37	3.94	1.44	3.47	3.47	6.29	1.24	1.52	2.37	3.93	1.43	1.93	3.47	6.27
1.10	1.24	1.52	2.37	3.94	1.44	3.47	3.47	6.29	1.24	1.52	2.37	3.93	1.43	1.93	3.47	6.27
1.20	1.24	1.52	2.37	3.94	1.44	3.47	3.47	6.29	1.26	1.52	2.37	3.93	1.43	1.93	3.47	6.27
1.30	1.28	1.52	2.37	3.94	1.44	3.47	3.47	6.29	1.27	1.54	2.65	5.17	1.49	1.93	3.47	6.27
1.40	1.30	1.60	2.60	4.99	1.49	3.47	3.47	6.29	1.30	1.60	2.61	4.91	1.47	1.93	3.47	6.27
1.50	1.29	1.60	2.60	4.92	1.47	3.47	3.47	6.29	1.29	1.59	2.61	4.85	1.52	1.93	3.47	6.27
1.60	1.29	1.60	2.60	4.88	1.53	3.47	3.47	6.29	1.29	1.59	2.61	4.85	1.52	1.93	3.47	6.27
1.70	1.29	1.60	2.60	4.88	1.53	3.47	3.47	6.29	1.29	1.59	2.61	4.85	1.52	1.93	3.96	6.27
1.80	1.30	1.60	2.60	4.88	1.53	3.47	3.47	6.29	1.29	1.59	2.61	4.85	1.52	2.06	3.96	7.93
1.90	1.30	1.60	2.60	4.88	1.53	3.47	3.47	6.29	1.29	1.59	2.61	4.85	1.52	2.06	3.96	7.93
2.00	1.30	1.60	2.60	4.88	1.53	3.47	3.47	7.98	1.29	1.59	2.61	4.85	1.52	1.93	3.96	7.93

17.4.5 Performance of the VSI EWMA-*R* Control Chart

Concerning the EWMA-R control chart, similar investigations were performed for determining the minimal *ATS* values achieved using the optimal VSI model. These minimal *ATS* values are summarized in Tables 17.16 and 17.17 for shifts $\tau \in \{0.6, 0.7, 0.8, 0.9, 0.95, 1.05, 1.1, 1.2, \ldots, 2\}$ and $n \in \{3, 5, 7, 9\}$. The values used for h_S are 0.5 and 0.1 time units. For comparison purposes, Tables 17.16 and 17.17 also show the minimal *ATS* of the FSI

Table 17.19 Optimal couples (λ^*, K^*) of the VSI EWMA-R for $n \in \{3, 5\}$, $\tau \in \{0.6, 0.7, 0.8, 0.9, 0.95, 1.05, 1.1, 1.2, \dots, 2\}$, $h_S \in \{0.1, 0.5\}$, $W = \{0.1, 0.3, 0.6, 0.9\}$, $ATS_0 = 370.4$

	$n = 3$															
	$h_S = 0.5$								$h_S = 0.1$							
	W								W							
	0.9		0.6		0.3		0.15		0.9		0.6		0.3		0.15	
τ	λ^*	K^*	λ^*	K^*	λ^*	K^*	λ^*	K^*	λ^*	K^*	λ^*	K^*	λ^*	K^*	λ^*	K^*
0.60	0.13	2.734	0.13	2.734	0.16	2.767	0.16	2.767	0.16	2.767	0.18	2.782	0.19	2.789	0.22	2.802
0.70	0.09	2.656	0.06	2.547	0.09	2.656	0.09	2.656	0.11	2.701	0.11	2.701	0.13	2.734	0.13	2.734
0.80	0.05	2.492	0.05	2.492	0.05	2.492	0.05	2.492	0.06	2.547	0.06	2.547	0.06	2.547	0.06	2.547
0.90	0.05	2.492	0.05	2.492	0.05	2.492	0.05	2.492	0.05	2.492	0.05	2.492	0.05	2.492	0.05	2.492
0.95	0.05	2.492	0.05	2.492	0.05	2.492	0.05	2.492	0.05	2.492	0.05	2.492	0.05	2.492	0.05	2.492
1.05	0.05	2.492	0.05	2.492	0.05	2.492	0.05	2.492	0.05	2.492	0.05	2.492	0.05	2.492	0.05	2.492
1.10	0.05	2.492	0.05	2.492	0.05	2.492	0.05	2.492	0.05	2.492	0.05	2.492	0.05	2.492	0.05	2.492
1.20	0.05	2.492	0.05	2.492	0.05	2.492	0.05	2.492	0.05	2.492	0.05	2.492	0.05	2.492	0.05	2.492
1.30	0.05	2.492	0.05	2.492	0.05	2.492	0.05	2.492	0.05	2.492	0.05	2.492	0.05	2.492	0.05	2.492
1.40	0.05	2.492	0.05	2.492	0.05	2.492	0.05	2.492	0.05	2.492	0.05	2.492	0.05	2.492	0.05	2.492
1.50	0.05	2.492	0.05	2.492	0.05	2.492	0.05	2.492	0.05	2.492	0.05	2.492	0.05	2.492	0.05	2.492
1.60	0.06	2.547	0.05	2.492	0.05	2.492	0.05	2.492	0.05	2.492	0.05	2.492	0.05	2.492	0.05	2.492
1.70	0.21	2.798	0.06	2.547	0.05	2.492	0.05	2.492	0.05	2.492	0.05	2.492	0.05	2.492	0.05	2.492
1.80	0.44	2.791	0.06	2.547	0.05	2.492	0.05	2.492	0.05	2.492	0.05	2.492	0.05	2.492	0.05	2.492
1.90	0.45	2.788	0.06	2.547	0.21	2.798	0.45	2.788	0.05	2.492	0.05	2.492	0.05	2.492	0.05	2.492
2.00	0.45	2.788	0.06	2.547	0.21	2.798	0.58	2.75	0.05	2.492	0.05	2.492	0.05	2.492	0.05	2.492
	$n = 5$															
	$h_S = 0.5$								$h_S = 0.1$							
	W								W							
	0.9		0.6		0.3		0.15		0.9		0.6		0.3		0.15	
τ	λ^*	K^*	λ^*	K^*	λ^*	K^*	λ^*	K^*	λ^*	K^*	λ^*	K^*	λ^*	K^*	λ^*	K^*
0.60	0.20	2.827	0.20	2.827	0.12	2.734	0.20	2.827	0.28	2.864	0.29	2.866	0.12	2.734	0.29	2.866
0.70	0.13	2.751	0.13	2.751	0.12	2.734	0.14	2.766	0.18	2.811	0.18	2.811	0.12	2.734	0.20	2.827
0.80	0.08	2.633	0.08	2.633	0.08	2.633	0.08	2.633	0.10	2.691	0.10	2.691	0.10	2.691	0.10	2.691
0.90	0.05	2.492	0.05	2.492	0.05	2.492	0.05	2.492	0.05	2.492	0.05	2.492	0.05	2.492	0.05	2.492
0.95	0.05	2.492	0.05	2.492	0.05	2.492	0.05	2.492	0.05	2.492	0.05	2.492	0.05	2.492	0.05	2.492
1.05	0.05	2.492	0.05	2.492	0.05	2.492	0.05	2.492	0.05	2.492	0.05	2.492	0.05	2.492	0.05	2.492
1.10	0.05	2.492	0.05	2.492	0.05	2.492	0.05	2.492	0.05	2.492	0.05	2.492	0.05	2.492	0.05	2.492
1.20	0.05	2.492	0.05	2.492	0.05	2.492	0.05	2.492	0.05	2.492	0.05	2.492	0.05	2.492	0.05	2.492
1.30	0.05	2.492	0.05	2.492	0.05	2.492	0.05	2.492	0.05	2.492	0.05	2.492	0.05	2.492	0.05	2.492
1.40	0.12	2.734	0.05	2.492	0.05	2.492	0.05	2.492	0.05	2.492	0.05	2.492	0.05	2.492	0.05	2.492
1.50	0.17	2.802	0.17	2.802	0.05	2.492	0.05	2.492	0.05	2.492	0.05	2.492	0.05	2.492	0.05	2.492
1.60	0.26	2.857	0.26	2.857	0.12	2.734	0.26	2.857	0.17	2.802	0.05	2.492	0.05	2.492	0.05	2.492
1.70	0.40	2.877	0.39	2.877	0.12	2.734	0.39	2.877	0.22	2.839	0.05	2.492	0.05	2.492	0.05	2.492
1.80	0.45	2.875	0.45	2.875	0.12	2.734	0.45	2.875	0.22	2.839	0.05	2.492	0.05	2.492	0.05	2.492
1.90	0.45	2.875	0.45	2.875	0.12	2.734	0.45	2.875	0.40	2.877	0.05	2.492	0.05	2.492	0.05	2.492
2.00	0.69	2.839	0.56	2.862	0.12	2.734	0.45	2.875	0.43	2.876	0.05	2.492	0.05	2.492	0.05	2.492

Table 17.20 Optimal couples (λ^*, K^*) of the VSI EWMA-R for $n \in \{7, 9\}$, $\tau \in \{0.6, 0.7, 0.8, 0.9, 0.95, 1.05, 1.1, 1.2, \ldots, 2\}$, $h_S \in \{0.1, 0.5\}$, $W = \{0.1, 0.3, 0.6, 0.9\}$, $ATS_0 = 370.4$

	$n=7$															
	$h_S = 0.5$								$h_S = 0.1$							
	W								W							
	0.9		0.6		0.3		0.15		0.9		0.6		0.3		0.15	
τ	λ^*	K^*	λ^*	K^*	λ^*	K^*	λ^*	K^*	λ^*	K^*	λ^*	K^*	λ^*	K^*	λ^*	K^*
0.60	0.27	2.880	0.26	2.876	0.10	2.696	0.25	2.871	0.38	2.907	0.38	2.907	0.10	2.696	0.35	2.902
0.70	0.17	2.812	0.18	2.822	0.10	2.696	0.22	2.854	0.22	2.854	0.24	2.866	0.10	2.696	0.24	2.866
0.80	0.11	2.719	0.11	2.719	0.10	2.696	0.11	2.719	0.11	2.719	0.12	2.740	0.10	2.696	0.15	2.788
0.90	0.05	2.492	0.05	2.492	0.05	2.492	0.05	2.492	0.05	2.492	0.05	2.492	0.05	2.492	0.05	2.492
0.95	0.05	2.492	0.05	2.492	0.05	2.492	0.05	2.492	0.05	2.492	0.05	2.492	0.05	2.492	0.05	2.492
1.05	0.05	2.492	0.05	2.492	0.05	2.492	0.05	2.492	0.05	2.492	0.05	2.492	0.05	2.492	0.05	2.492
1.10	0.05	2.492	0.05	2.492	0.05	2.492	0.05	2.492	0.05	2.492	0.05	2.492	0.05	2.492	0.05	2.492
1.20	0.05	2.492	0.05	2.492	0.05	2.492	0.05	2.492	0.05	2.492	0.05	2.492	0.05	2.492	0.05	2.492
1.30	0.10	2.696	0.05	2.492	0.05	2.492	0.05	2.492	0.05	2.492	0.05	2.492	0.05	2.492	0.05	2.492
1.40	0.21	2.847	0.21	2.847	0.10	2.696	0.14	2.774	0.14	2.774	0.05	2.492	0.05	2.492	0.05	2.492
1.50	0.30	2.890	0.29	2.887	0.10	2.696	0.21	2.847	0.20	2.840	0.05	2.492	0.05	2.492	0.05	2.492
1.60	0.37	2.905	0.37	2.905	0.10	2.696	0.37	2.905	0.33	2.898	0.05	2.492	0.05	2.492	0.05	2.492
1.70	0.37	2.905	0.37	2.905	0.10	2.696	0.37	2.905	0.37	2.905	0.05	2.492	0.05	2.492	0.05	2.492
1.80	0.53	2.911	0.52	2.911	0.10	2.696	0.37	2.905	0.37	2.905	0.05	2.492	0.05	2.492	0.05	2.492
1.90	0.58	2.909	0.58	2.909	0.10	2.696	0.37	2.905	0.37	2.905	0.05	2.492	0.05	2.492	0.05	2.492
2.00	0.64	2.904	0.62	2.906	0.10	2.696	0.37	2.905	0.52	2.911	0.05	2.492	0.05	2.492	0.37	2.905

	$n=9$															
	$h_S = 0.5$								$h_S = 0.1$							
	W								W							
	0.9		0.6		0.3		0.15		0.9		0.6		0.3		0.15	
τ	λ^*	K^*	λ^*	K^*	λ^*	K^*	λ^*	K^*	λ^*	K^*	λ^*	K^*	λ^*	K^*	λ^*	K^*
0.60	0.35	2.916	0.35	2.916	0.09	2.670	0.30	2.901	0.41	2.926	0.40	2.925	0.40	2.925	0.34	2.913
0.70	0.21	2.854	0.21	2.854	0.09	2.670	0.21	2.854	0.27	2.889	0.28	2.894	0.28	2.894	0.29	2.898
0.80	0.11	2.722	0.14	2.777	0.09	2.670	0.14	2.777	0.14	2.777	0.15	2.792	0.15	2.792	0.16	2.805
0.90	0.05	2.492	0.05	2.492	0.05	2.492	0.05	2.492	0.06	2.551	0.06	2.551	0.06	2.551	0.06	2.551
0.95	0.05	2.492	0.05	2.492	0.05	2.492	0.05	2.492	0.05	2.492	0.05	2.492	0.05	2.492	0.05	2.492
1.05	0.05	2.492	0.05	2.492	0.05	2.492	0.05	2.492	0.05	2.492	0.05	2.492	0.05	2.492	0.05	2.492
1.10	0.05	2.492	0.05	2.492	0.05	2.492	0.05	2.492	0.05	2.492	0.05	2.492	0.05	2.492	0.05	2.492
1.20	0.07	2.599	0.05	2.492	0.05	2.492	0.05	2.492	0.05	2.492	0.05	2.492	0.05	2.492	0.05	2.492
1.30	0.13	2.761	0.12	2.743	0.07	2.599	0.07	2.599	0.13	2.761	0.05	2.492	0.05	2.492	0.05	2.492
1.40	0.20	2.846	0.20	2.846	0.09	2.670	0.20	2.846	0.19	2.837	0.05	2.492	0.05	2.492	0.05	2.492
1.50	0.33	2.911	0.33	2.911	0.09	2.670	0.32	2.908	0.32	2.908	0.05	2.492	0.05	2.492	0.05	2.492
1.60	0.34	2.913	0.34	2.913	0.09	2.670	0.34	2.913	0.34	2.913	0.05	2.492	0.05	2.492	0.05	2.492
1.70	0.50	2.933	0.50	2.933	0.09	2.670	0.34	2.913	0.34	2.913	0.05	2.492	0.07	2.599	0.05	2.492
1.80	0.57	2.934	0.57	2.934	0.09	2.670	0.34	2.913	0.50	2.933	0.48	2.932	0.07	2.599	0.34	2.913
1.90	0.63	2.933	0.62	2.933	0.09	2.670	0.34	2.913	0.55	2.934	0.52	2.934	0.07	2.599	0.34	2.913
2.00	0.68	2.931	0.67	2.932	0.09	2.670	0.34	2.913	0.59	2.934	0.05	2.492	0.07	2.599	0.34	2.913

EWMA-R (column $h_L = 1$). Like the VSI EWMA-S^2 control chart, the results clearly indicate that the VSI EWMA-R control chart outperforms the FSI scheme for all considered shifts of variability since the VSI model gives a signal earlier than the FSI model. For example, for $n = 5$, $h_S = 0.5$ and $W = 0.6$ we have $ATS^* = 63.4$ when $\tau = 0.9$, while for the FSI model we have $ATS^* = 75.0$. When $\tau = 1.2$, we have $ATS^* = 16.6$ for the VSI EWMA-R control chart, while for the FSI model we have $ATS^* = 22.5$. Table 17.18 shows the optimal long sampling interval h_L^* for several combinations of n, W, h_S and τ. Finally, Tables 17.19 and 17.20 summarize the optimal couples (λ^*, K^*).

17.5 Conclusions

This chapter presented several EWMA control charts, both with static or adaptive design parameters, as effective means to monitor the process variability, involving both process position and dispersion. The EWMA control charts are a tool of statistical process control widely adopted in the manufacturing environments, due to their sensitivity in the detection of process drifts caused by special causes influencing variability. EWMA charts outperform the statistical performance of traditional Shewhart control charts thanks to the definition of the statistic to be monitored, which contains information about the past process history: this translates into a faster response on the chart to the presence of an out-of-control condition. Reducing the number of samples to be taken between the occurrence of a special cause and its detection on the control chart is very important because this allows the probability of nonconforming units to be controlled. The average run length (*ARL*), defined as the expected number of samples to be taken before a signal from the chart, was assumed as a quantitative parameter to measure the speed of the chart in revealing the occurrence of a special cause. Through this parameter, different control chart schemes can be directly compared assuming as a common constraint the same probability to signal for a false alarm. To evaluate the *ARL* of static EWMAs, two procedures were presented in this chapter: an approach based on the numerical integration of a Fredholm equation and another based on an approximate discrete Markov-chain model. The *ARL* evaluation of the adaptive EWMAs was performed through the Markov chain, which, in this case, allows for an easy mathematical formulation to be modeled. Traditionally, static and adaptive EWMA charts have been implemented in order to monitor the process position with respect to a particular target value: EWMAs for the process mean and median monitoring have been developed in the literature and compared each other or with Shewhart schemes for the sample mean or median. Here, an extensive set of results are presented for the out-of-control *ARL* of these charts: the analysis of the data shows how the static EWMA-$\bar{X}$ always outperforms the static EWMA-$\tilde{X}$ and the corresponding Shewhart scheme for a wide range of assumed drifts, whatever the sample size. Therefore, the adoption of the EWMA-$\bar{X}$ is suggested to the practitioner whenever small process drifts must be detected. However, in statistical quality control the monitoring of

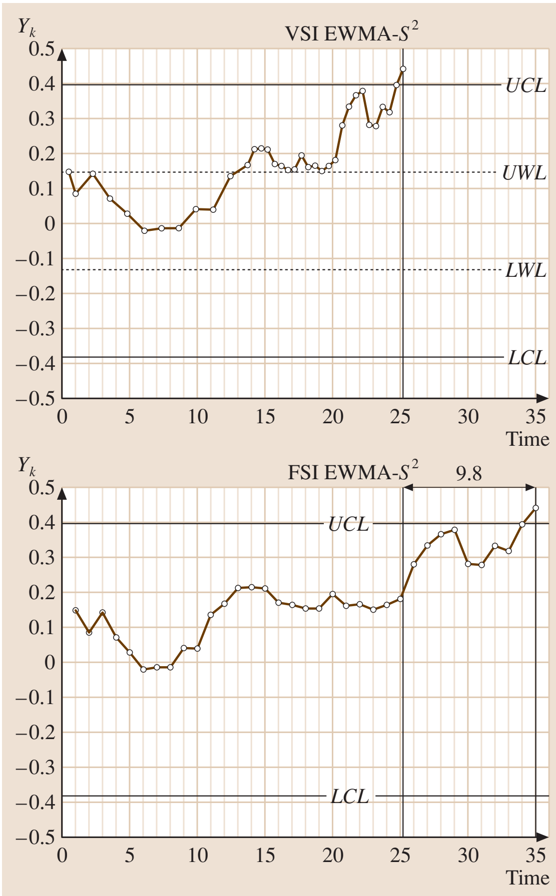

Fig. 17.18 FSI and VSI EWMA-S^2 control chart corresponding to the data in Table 17.15

the process dispersion is equally important as the position, which can be conducted by applying EWMAs to statistics based on the sample dispersion. A survey of EWMAs for monitoring the sample standard deviation S, sample variance S^2 and sample range R was reported in this chapter. The investigated charts work on logarithmic transformations of the measures of dispersion to cope with a variable approximately normally distributed: the formulas adopted to achieve this transformed variable are widely reported throughout the text. The reason for this approach lies in the possibility of managing charts characterized by symmetrical limits, which is common practice in industrial applications to simplify the operator's tasks in the management of the chart. The selected logarithmic transformations work well for all the considered statistics and allow for a direct comparison of the statistical properties of the three charts investigated. The *ARL* computation, optimization and comparison for the three static EWMAs allowed us to demonstrate that the EWMA-S^2 always outperforms both the EWMA-S and EWMA-R when the occurrence of a special cause results in an increase in the dispersion of the data; i.e., when a process is monitored and a deterioration in process repeatability is expected, the EWMA-S^2 is suitable to detect it. Otherwise, if a reduction in process dispersion is expected, for example after a machine maintenance intervention or technological improvement, then the EWMA-R or EWMA-S should be used: in particular, for small sample sizes, ($n \leq 5$), implementing the EWMA monitoring the sample range R is statistically more correct than the EWMA-S, due to the scarce number of measures adopted to evaluate the dispersion statistic. When $n > 5$, the EWMA-S should be used. A further step in the analysis involved the investigation of the adaptive version of the EWMA-S^2 and EWMA-R charts. These adaptive charts have a sampling frequency which is a function of the position of the last plotted point on the chart. The underlying idea is that, when a point is plotted near to the control limits, a possible special cause could be occurring, even if the chart still has not signaled an out-of-control condition; if this is the case, then the next sample should be taken after a shorter time interval. For this reason the variable sampling interval versions of EWMA-S^2 and EWMA-R have been designed and investigated; the EWMA control interval was divided into three zones: a point falling within the central zone, containing the central line of the chart, calls for a longer sampling interval, whereas a point plotted within one of the two external zones included between the central zone and the control limits calls for a shorter time interval. Due to the variability of the time between two samples, the statistical efficiency of these charts was not measured through the *ARL* but through the average time to signal *ATS*. *ATS*s were computed for several sample sizes and expected shifts in process dispersion through the approximate Markov-chain model. For each of the two investigated charts several tables were reported, including the optimal *ATS*s, a comparison with the corresponding static schemes and the values of the optimal parameters. The results show that the variable sampling interval charts always statistically outperform the static charts; furthermore, the differences between S^2 and R found for the static schemes also occur for the adaptive versions: therefore, when increases in process dispersion are expected, the VSI EWMA-S^2 should be used, otherwise the VSI EWMA-R represents the best choice. Finally, it must be argued that EWMA schemes represent a more powerful tool than the traditional Shewhart control charts when process variability is to be monitored, enhancing their statistical properties through the possibility of varying the sampling frequency is effective, whichever the entity of the drift. As a consequence future research should be devoted to the development of adaptive schemes involving the possibility of changing sample size or both sample frequency and sample size.

References

17.1 S. W. Roberts: Control chart tests based on geometric moving averages, Technometrics **1**(3), 239–250 (1959)

17.2 P. B. Robinson, T. Y. Ho: Average run lengths of geometric moving average charts by numerical methods, Technometrics **20**(1), 85–93 (1978)

17.3 S. V. Crowder: A simple method for studying run-length distributions of exponentially weighted moving average charts, Technometrics **29**(4), 401–407 (1987)

17.4 S. V. Crowder: Design of exponentially weighted moving average schemes, J. Qual. Technol. **21**(3), 155–162 (1989)

17.5 J. M. Lucas, M. S. Saccucci: Exponentially weighted moving average control schemes: Properties and enhancements, Technometrics **32**(1), 1–12 (1990)

17.6 S. H. Steiner: Exponentially weighted moving average control charts with time varying control limits and fast initial response, J. Qual. Technol. **31**, 75–86 (1999)

17.7 A. W. Wortham, L. J. Ringer: Control via exponential smoothing, Logist. Rev. **7**(32), 33–40 (1971)

17.8 A. L. Sweet: Control charts using coupled exponentially weighted moving averages, IIE Trans. **18**, 26–33 (1986)

17.9 C. H. Ng, K. E. Case: Development and evaluation of control charts using exponentially weighted moving averages, J. Qual. Technol. **21**(4), 242–250 (1989)

17.10 S. V. Crowder, M. D. Hamilton: An EWMA for monitoring a process standard deviation, J. Qual. Technol. **24**(1), 12–21 (1992)

17.11 M. D. Hamilton, S. V. Crowder: Average run lengths of EWMA control charts for monitoring a process standard deviation, J. Qual. Technol. **24**(1), 44–50 (1992)

17.12 J. F. MacGregor, T. J. Harris: The exponentially weighted moving variance, J. Qual. Technol. **25**(2), 106–118 (1993)

17.13 F. F. Gan: Joint monitoring of process mean and variance using exponentially weighted moving average control charts, Technometrics **37**, 446–453 (1995)

17.14 R. W. Amin, H. Wolff, W. Besenfelder, R. Jr. Baxley: EWMA control charts for the smallest and largest observations, J. Qual. Technol. **31**, 189–206 (1999)

17.15 C. W. Lu, M. R. Jr. Reynolds: Control charts for monitoring the mean and variance of autocorrelated processes, J. Qual. Technol. **31**, 259–274 (1999)

17.16 C. A. Acosta-Mejia, J. J. Jr. Pignatiello, B. V. Rao: A comparison of control charting procedures for monitoring process dispersion, IIE Trans. **31**, 569–579 (1999)

17.17 P. Castagliola: *An EWMA control chart for monitoring the logarithm of the process sample variance*, *Proc. International Conference on Industrial Engineering and Production Management* (FUCAM, Mons 1999) pp. 371–377

17.18 W. H. Press, S. A. Teukolsky, W. T. Vetterling, B. P. Flannery: *Numerical Recipes in C* (Cambridge Univ. Press, Cambridge 1988)

17.19 D. Brook, D. A. Evans: An approach to the probability distribution of CUSUM run length, Biometrika **59**(3), 539–549 (1972)

17.20 P. Castagliola: An $(\tilde{X}/R)$-EWMA control chart for monitoring the process sample median, Int. J. Reliab. Qual. Safety Eng. **8**(2), 123–125 (2001)

17.21 P. Castagliola: Approximation of the normal sample median distribution using symmetrical Johnson S_U distributions: Application to quality control, Commun. Stat. Simul. Comput. **27**(2), 289–301 (1998)

17.22 G. E. Box, W. G. Hunter, J. S. Hunter: *Statistics for Experimenters* (Wiley, New York 1978)

17.23 N. L. Johnson, S. Kotz, N. Balakrishnan: *Continuous Univariate Distributions* (Wiley, New York 1994)

17.24 P. Castagliola: A New S^2-EWMA Control Chart for Monitoring the Process Variance, Qual. Reliab. Eng. Int. **21**(8) (2005)

17.25 A. Stuart, J. K. Ord: *Kendall's Advanced Theory of Statistics*, Vol. 1 (Edward Arnold, London 1994)

17.26 P. Castagliola: *A New EWMA Control Chart for Monitoring the Process Standard-Deviation*, *Proc. 6th ISSAT International Conference on Reliability and Quality in Design* (ISSAT, New Brunswick 2000) pp. 233–237

17.27 P. Castagliola: A R-EWMA control chart for monitoring the process range, Int. J. Reliab. Qual. Safety Eng. **12**(1), 31–49 (2005)

17.28 M. R. Reynolds Jr, R. W. Amin, J. Arnold, J. Nachlas: $\bar{X}$ charts with variable sampling intervals, Technometrics **30**(2), 181–192 (1988)

17.29 M. R. Reynolds Jr, R. W. Amin, J. Arnold: CUSUM chart with variable sampling intervals, Technometrics **32**(4), 371–384 (1990)

17.30 G. Runger, J. J. Pignatiello Jr: Adaptive sampling for process control, J. Qual. Technol. **23**(2), 135–155 (1991)

17.31 M. S. Saccucci, R. W. Amin, J. Lucas: Exponentially weighted moving average control scheme with variable sampling intervals, Commun. Stat. Simul. Comput. **21**(3), 627–657 (1992)

17.32 M. R. Reynolds Jr: Shewhart and EWMA variable sampling interval control charts with sampling at fixed times, J. Qual. Technol. **28**(2), 199–212 (1996)

17.33 I. Chengular, J. Arnolds, M. R. Reynolds Jr.: Variable sampling intervals for multiparameter Shewhart charts, Commun. Stat. Theory Methods **18**, 1769–1792 (1993)

17.34 M. R. Reynolds Jr., Z. Stoumbos: Monitoring the process mean and variance using individual observations and variable sampling intervals, J. Qual. Technol. **33**(2), 181–205 (2001)

17.35 M. Reynolds: Evaluation properties of variable sampling interval control charts, Sequential Anal. **14**(1), 59–97 (1995)

17.36 P. Castagliola, G. Celano, S. Fichera, F. Giuffrida: A variable sampling interval S^2-EWMA control chart for monitoring the process variance, Int. J. Technol. Manage. (2006) to be published